

AD-A194 114 A STUDY OF THE FLOATING ROLLER PEEL TEST FOR ADHESIVES
(U) DAYTON UNIV OH RESEARCH INST R D KEMP ET AL.
OCT 87 UDR-TR-87-82 AFMIL-TR-87-4082 F33615-85-C-5094

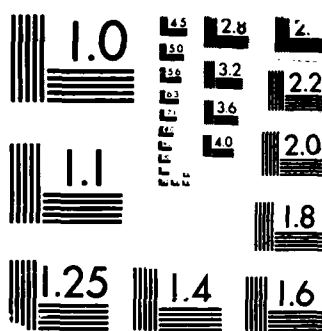
A STUDY OF THE FLOATING ROLLER PEEL TEST FOR ADHESIVES
(U) DAYTON UNIV OH RESEARCH INST R D KEMP ET AL.
OCT 87 UDR-TR-87-82 AFMIL-TR-87-4002 F33615-85-C-5094

1/1

UNCLASSIFIED

F/G 11/1

NL

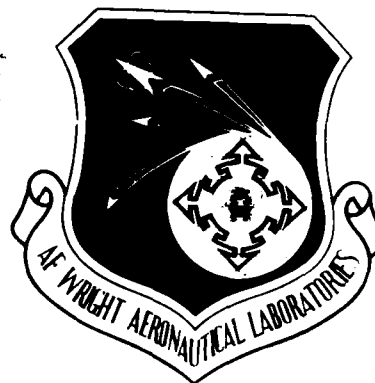


MICROCOPY RESOLUTION TEST CHART
 NATIONAL BUREAU OF STANDARDS-1963-A

AD-A194 114

AFWAL-TR-87- 4082

DTIC FILE COPY



A STUDY OF THE FLOATING ROLLER PEEL TEST
FOR ADHESIVES

R. David Kemp
Robert A. Brockman
Gregory J. Stenger

University of Dayton
Research Institute
300 College Park Avenue
Dayton, OH 45469

DTIC
ELECTE
APR 26 1988
S D

OCTOBER 1987

Interim Technical Report - January 1986-June 1987

Approved for public release; distribution unlimited

MATERIALS LABORATORY
AIR FORCE WRIGHT AERONAUTICAL LABORATORIES
AIR FORCE SYSTEMS COMMAND
WRIGHT-PATTERSON AIR FORCE BASE, OHIO 45433-6533

88 4 25 027

UNCLASSIFIED

SECURITY CLASSIFICATION OF THIS PAGE

REPORT DOCUMENTATION PAGE

1a. REPORT SECURITY CLASSIFICATION Unclassified			1b. RESTRICTIVE MARKINGS	
2a. SECURITY CLASSIFICATION AUTHORITY			3. DISTRIBUTION/AVAILABILITY OF REPORT Approved for public release; distribution unlimited.	
2b. DECLASSIFICATION/DOWNGRADING SCHEDULE				
4. PERFORMING ORGANIZATION REPORT NUMBER(S) UDR-TR-87-82			5. MONITORING ORGANIZATION REPORT NUMBER(S) AFWAL-TR-87-4082	
6a. NAME OF PERFORMING ORGANIZATION University of Dayton Research Institute		6b. OFFICE SYMBOL (If applicable)	7a. NAME OF MONITORING ORGANIZATION Air Force Wright Aeronautical Laboratories Materials Laboratory (AFWAL/MLSE)	
6c. ADDRESS (City, State and ZIP Code) 300 College Park Avenue Dayton, OH 45469			7b. ADDRESS (City, State and ZIP Code) Wright-Patterson Air Force Base, OH 45433-6533	
8a. NAME OF FUNDING/SPONSORING ORGANIZATION		8b. OFFICE SYMBOL (If applicable)	9. PROCUREMENT INSTRUMENT IDENTIFICATION NUMBER F33615-85-C-5094	
8c. ADDRESS (City, State and ZIP Code)			10. SOURCE OF FUNDING NOS.	
			PROGRAM ELEMENT NO. 62102F	PROJECT NO. 2418
11. TITLE (Include Security Classification) A STUDY OF THE FLOATING ROLLER PEEL TEST FOR ADHESIVES				
12. PERSONAL AUTHOR(S) R. David Kemp, Robert A. Brockman, and Gregory J. Stenger				
13a. TYPE OF REPORT Technical Interim	13b. TIME COVERED FROM 1/86 TO 6/87		14. DATE OF REPORT (Yr., Mo., Day) October 1987	
15. PAGE COUNT 65				
16. SUPPLEMENTARY NOTATION				
17. COSATI CODES			18. SUBJECT TERMS (Continue on reverse if necessary and identify by block number)	
FIELD	GROUP	SUB. GR.	Floating Roller Peel, Peel Strength, Adhesive, Adherend Stiffness, Adherend, Bond Strength (cont. on other side)	
11	01			
19. ABSTRACT (Continue on reverse if necessary and identify by block number) Peel testing of adhesives has not been extensively evaluated using analytical methods. Current test methods cannot discriminate between the work required to deform the adherend and the work needed to fail the adhesive. In some cases, the work required to bend the adherend is much greater than that required for adhesive failure. Further complications arise from inconsistent failure modes. Each of these circumstances can result in invalid or meaningless data. The objective of this investigation was to evaluate and improve the Floating Roller Peel Test (ASTM D3167) to enhance the accuracy and significance of the test results and to develop an analytical technique for calculating the work required to deform the adherend. The technique developed enables the analyst to determine the percentage of the total work needed to fail the adhesive and thus aid in evaluating adhesive performance. An analytical model was developed as part of this investigation to predict the work required (Continued on other side)				
20. DISTRIBUTION/AVAILABILITY OF ABSTRACT UNCLASSIFIED/UNLIMITED <input checked="" type="checkbox"/> SAME AS RPT. <input type="checkbox"/> DTIC USERS <input type="checkbox"/>			21. ABSTRACT SECURITY CLASSIFICATION Unclassified	
22a. NAME OF RESPONSIBLE INDIVIDUAL Robert Urzi			22b. TELEPHONE NUMBER (Include Area Code) (513) 255-7481	22c. OFFICE SYMBOL AFWAL/MLSE

UNCLASSIFIED

SECURITY CLASSIFICATION OF THIS PAGE

18. SUBJECT TERMS (Continued)

Elastic,	Flexible .
Plastic,	UDRI Fixture
Rigid .	Failure Mode ←

19. ABSTRACT (Continued)

to deform the adherend, and the analytical results agree with experimental data. In addition, design modifications were made to the ASTM test fixture to improve the quality of the measured peel data. The new fixture was found to be superior to the ASTM fixture for adhesives exhibiting low peel strength.

UNCLASSIFIED

PREFACE

This summary report covers work performed during the period 3 January 1986 to 9 June 1987 under Air Force Contract F33615-85-C-5094. The contract was initiated under Project Number 2418. The work was administered under the direction of the Systems Support Division of the Air Force Wright Aeronautical Laboratories/Materials Laboratory, Wright-Patterson Air Force Base, Ohio. Mr. Robert Urzi (AFWAL/MLSA) acted as Project Engineer.

This work was conducted under the general supervision of Mr. D. Gerdeman, Project Supervisor. The Principal Investigator for this program was Mr. D. Robert Askins. The project reported here was carried out by the author, Mr. R. David Kemp. Major contributors to the effort were Dr. Robert Brockman, who provided guidance and ideas in the development of the analytical model; Mr. Greg Stenger, who provided ideas and guidance in the overall project work; and to Messrs. Mike Bouchard and Robert Askins, who contributed useful discussions. Appreciation is also extended to Mr. Dee Pike for specimen preparation, and Messrs. Don Byrge, Perry Wagner, and Pete Muth for the specimen testing. The author especially wishes to thank Mr. Robert Askins for his extensive assistance in reviewing and editing this report.



Accession For	
NTIS CRA&I	<input checked="checked" type="checkbox"/>
DTIC TAB	<input type="checkbox"/>
Unannounced	<input type="checkbox"/>
Justification	
By	
Distribution/	
Availability Codes	
Dist	Avail and/or Special
A-1	

TABLE CONTENTS

<u>SECTION</u>		<u>PAGE</u>
1	INTRODUCTION	1
2	BACKGROUND	6
3	ANALYTICAL APPROACH FOR ANALYSIS OF ADHEREND DEFORMATION	7
4	ANALYTICAL RESULTS FOR ADHEREND DEFORMATION	16
5	TEST FIXTURE MODIFICATION	20
6	EXPERIMENTAL RESULTS	27
7	CONCLUSIONS	38
8	RECOMMENDATIONS	39
	REFERENCES	41
	NOMENCLATURE	42
	APPENDIX A: COMPUTER ANALYSIS OF PEEL PROCESS	45
	APPENDIX B: GUIDELINES FOR USE OF UDRI FIXTURE	57

LIST OF ILLUSTRATIONS

<u>FIGURE</u>		<u>PAGE</u>
1	Comparison of Well and Poorly Behaved D3167 Floating Roller Peel Tests	2
2	Floating Roller Peel Tests for a Strong and Weak Adhesive	3
3	Geometry of Flexible Adherend Deformation During ASTM D3167 Test	8
4	Loading Path for a Typical Point Undergoing Plastic Deformation in the Adherend	10
5	Geometry of Adherend	12
6	Analytical Results for the Flexible Adherend Deformation for 6061-T6 Aluminum	17
7	Analytical Results for the Flexible Adherend Deformation for 2024-T3 Aluminum	19
8	UDRI Test Fixture	20
9	Specimen Design with Intermittent Adherend Bonding	21
10	Expected Peel Results for Double-Faced Intermittent Tape	22
11	Peel Test Results with Intermittent Tape	23
12	Comparison of Measured Peel Strengths of a Weak Adhesive at -67°F	25
13	Comparison of Experimental Work Per Unit Length with Results from Analytical Model for 6061-T6	31
14	Comparison of Experimental Work Per Unit Length with Results from Analytical Model for 2024-T3	32
15	Peel Failure Modes for a Strong Adhesive	36
16	UDRI Test Fixture	58
17	Detailed Drawing of UDRI Test Fixture	59

LIST OF TABLES

<u>TABLE</u>		<u>PAGE</u>
1	Comparison of Analytical and Experimental Peel Loads for Various Adherend Stiffnesses	28
2	Comparison of Analytical and Experimental Peel Loads for Various Adherend Stiffnesses	29
3	Experimental Peel Results for Specimens Bonded with a Low Peel Strength Adhesive	34
4	Experimental Peel Results for Specimens Bonded with a High Peel Strength Adhesive	35

SECTION 1

INTRODUCTION

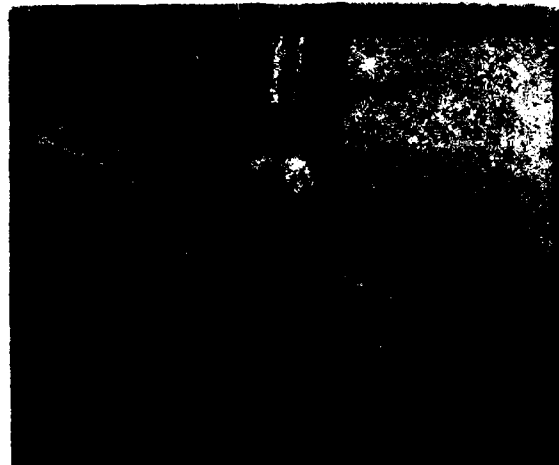
Peel testing to determine adhesive bond strength is useful for quality control, as well as an evaluation aid for adhesive selection. Two commonly used peel tests are the Climbing Drum Peel Test, ASTM D1781 [1], and the Floating Roller Peel Test, ASTM D3167 [2]. The climbing drum peel test is used primarily for bonded sandwich structure. It can, however, be used to evaluate metal-to-metal bonds. The floating roller peel test is used exclusively for metal-to-metal bonds.

In Method D3167, the peel strength is determined by dividing the average peeling load by the specimen width. This procedure does not distinguish quantitatively between the percentage of the load required to fail the adhesive and the percentage of the load required to deform the flexible adherend. Rather, the total load necessary to both deform the flexible adherend and fail the adhesive is used to calculate the peel strength. It is apparent that variations in properties of the flexible adherend (yield stress, stiffness, thickness, etc.) will influence the test results. For this reason, this test method can at best be used for direct comparison of different adhesives only when specimen construction and conditions are identical. Even then, in the case of low peel strength adhesives, the load necessary to deform the flexible adherend is by far the major contributor to the total measured load and the ability of the procedure to discriminate between weak adhesives becomes minimal. Other problems also occur when weak adhesives are tested in accordance with test Method D3167. These are related to the fact that the test fixture does not adequately constrain the specimen. For small ratios of adhesive peel strength to adherend stiffness, the unconstrained end of the specimen will rise, and the test fixture will rotate to compensate for the change in position of the specimen. The adhesive will begin to fail in cleavage rather than peel, causing the failure to occur well before the adherend translates over the

roller. Figure 1 illustrates the two extremes in peel behavior encountered with the Floating Roller Peel Test (D3167).



a) Well Behaved Peel Test, Typical of High Peel Strength Adhesive.



b) Poorly Behaved Peel Test, Typical of Low Peel Strength Adhesive.

Figure 1: Comparison of Well and Poorly Behaved D3167 Floating Roller Peel Tests

The measured loads will be spiked and erratic, characteristic of crack jump/arrest behavior and one will frequently observe a load pattern in which the overall load recording diminishes continuously from start to finish of the test, with no portion ever approaching a constant or level load behavior. Figure 2 illustrates Floating Roller Peel Test results for both high and low peel strength adhesives. The D3167 specification cites the fact that "direct comparison of different adhesives can be made only when the angle of peel is identical." The operator must ascertain that the flexible adherend is bending smoothly over the roller and not at some irregular angle. Some analysts attempt to enforce this condition by manually constraining the free end of the specimen with finger pressure to prevent the end from rising. This external load does affect the test results recorded by the autograph machine. Figures 2c illustrates this effect for the same adhesive that was tested unconstrained in Figure 2b.

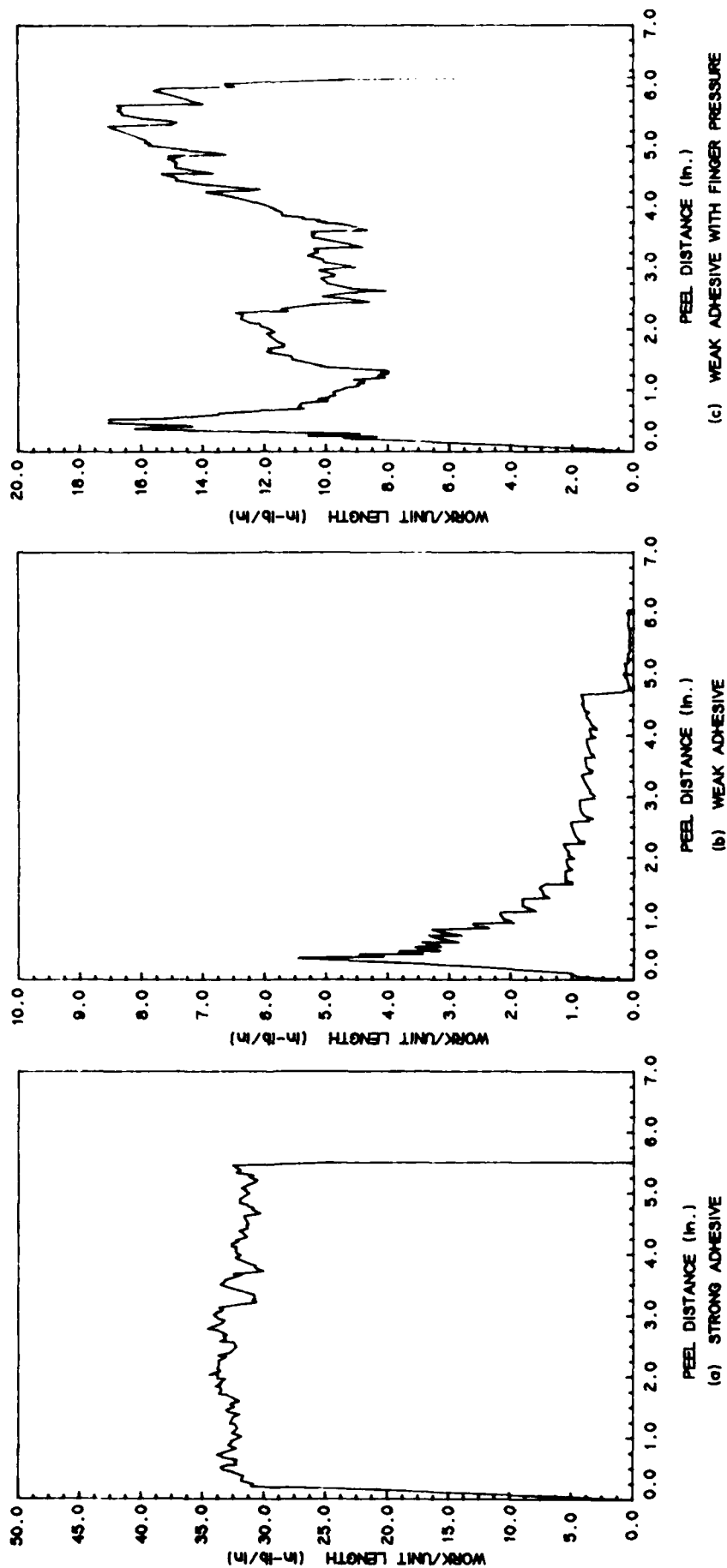


FIGURE 2 - FLOATING ROLLER PEEL TESTS FOR A STRONG AND WEAK ADHESIVE

When this type of failure behavior occurs, it becomes impossible to compare different adhesives because the peel angle changes and the data cannot be considered accurate. Thus, while the stated purpose in the introduction to D3167 is "to provide for the determination of the metal-to-metal peel strength of adhesives by a method that will provide good reproducibility at low, as well as high, strength levels...", this is not achieved in the case of low peel strength adhesives.

In the case of Method D1781, the determination of peel strength (or torque) requires that one first calibrate the test apparatus by inserting "...a piece of material of the same composition, properties, and dimensions as the adherend to be peeled" in the test fixture and measure the load necessary to roll the drum upward on the adherend. This calibration load compensates for the load necessary to bend the adherend and to overcome the resisting torque of the test fixture, and must be subtracted from the total load measured during the peel test. It is not uncommon for the calibration load to constitute 90% or more of the total load measured during a peel test. Since the load necessary to fail the adhesive bond can be such a small portion of the total measured load, a relatively small inaccuracy or uncertainty in the calibration load leads to a relatively high uncertainty in the calculated peel strength. In addition, we have been unable to identify any studies wherein the effect of various adherend characteristics (such as thickness or stiffness) and fixture dimensions (such as drum radius) on calculated peel resistance of adhesives has been reported.

As a result of these deficiencies with current peel test procedures, an investigation was undertaken with an objective of improving the accuracy and consistency of test methods used to measure adhesive peel strength. The primary focus was on the floating roller peel test, since it was the more difficult of the two to analyze. An analytical model was developed which provides a means of interpreting and comparing test data independent of the test specimen construction. Using the analytical model, the analyst will be able to distinguish between the

percentage of the peel load required to fail the adhesive and the percentage needed to deform the flexible adherend. The model was found to exhibit good accuracy for a series of tests which encompassed several different flexible adherend thicknesses and materials. The University of Dayton Research Institute (UDRI) made design modifications to the ASTM peel test fixture described in D3167. The new UDRI test fixture eliminates the problems mentioned above and is able to collect meaningful data at any test condition.

Before continuing, it is important to define terms that describe measured results. The terms peel load and peel force can be used interchangeably. These terms represent the force (measured in newtons or pounds) applied to the flexible adherend to pull the test specimen through the apparatus. Peel strength, as mentioned earlier, is defined as the average peel load divided by the specimen width. Work per unit length is the same as the peel load. Since the autographic recorder traverses at the same rate as the crosshead speed of the test apparatus, the recorded curve represents the peel load versus the distance peeled. The area under this curve denotes the total work performed during the test. The area under one unit of length on the autograph curve represents the work per unit length, which in turn, corresponds to the measured peel load. Note that each of these terms can be used to describe measured results for either the adhesive and/or adherend.

SECTION 2

BACKGROUND

Several people have studied the mechanics of peel adhesion, including Kaible [3,4] and Bikerman [5] with the most extensive being that of Kaible. In the development of their respective theories, each derived equations which approximated the peel force required to produce a cohesive failure. All studied the effects of different peel angles on the peel strength of various adhesives. In addition, Kaible developed his theory to investigate the cleavage and shear bond stresses during the unbonding process, and to examine the effect of peel rate and temperature upon adhesive peel strengths. Each theory, however, was based on the assumption that the flexible adherend remained elastic during the peel process. It is apparent that this is not the case for peel tests which use metallic adherends because the flexible adherend deforms plastically. Furthermore, their theories are not able to distinguish the force required to fail the adhesive from that required to deform the adherend, which leads back to the problems mentioned in Section 1. Although their work may be of some benefit when modeling adhesives, a more extensive analysis is required to model the mechanics of the adherend deformation.

SECTION 3

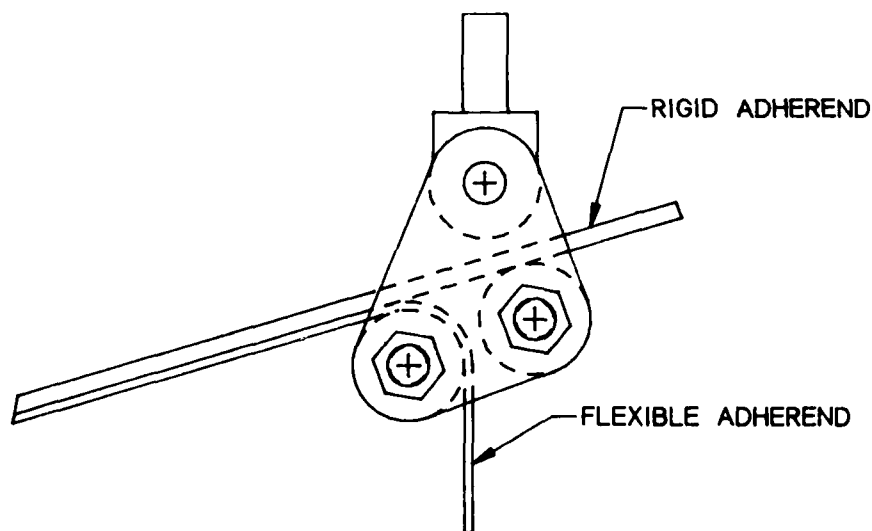
ANALYTICAL APPROACH FOR ANALYSIS OF ADHEREND DEFORMATION

During a floating roller peel test, the flexible adherend should conform to the geometry of the roller when peeled from the rigid adherend, as shown in Figure 3a. Test specimens are pulled through the fixture at a constant rate of six inches per minute. Since the peeling occurs at a low rate, the effect of the inertial forces is minimal and can be neglected, thus the analysis can be developed by treating the deformation of the adherend as an irreversible quasistatic process [6]. Under this assumption, time becomes an independent variable where it is understood to be always increasing and represents various states of deformation of the flexible adherend. An energy approach can then be used to develop an analytical model to describe the flexible adherend as it undergoes elastic and inelastic deformation. The model developed in this report is based upon the following assumptions:

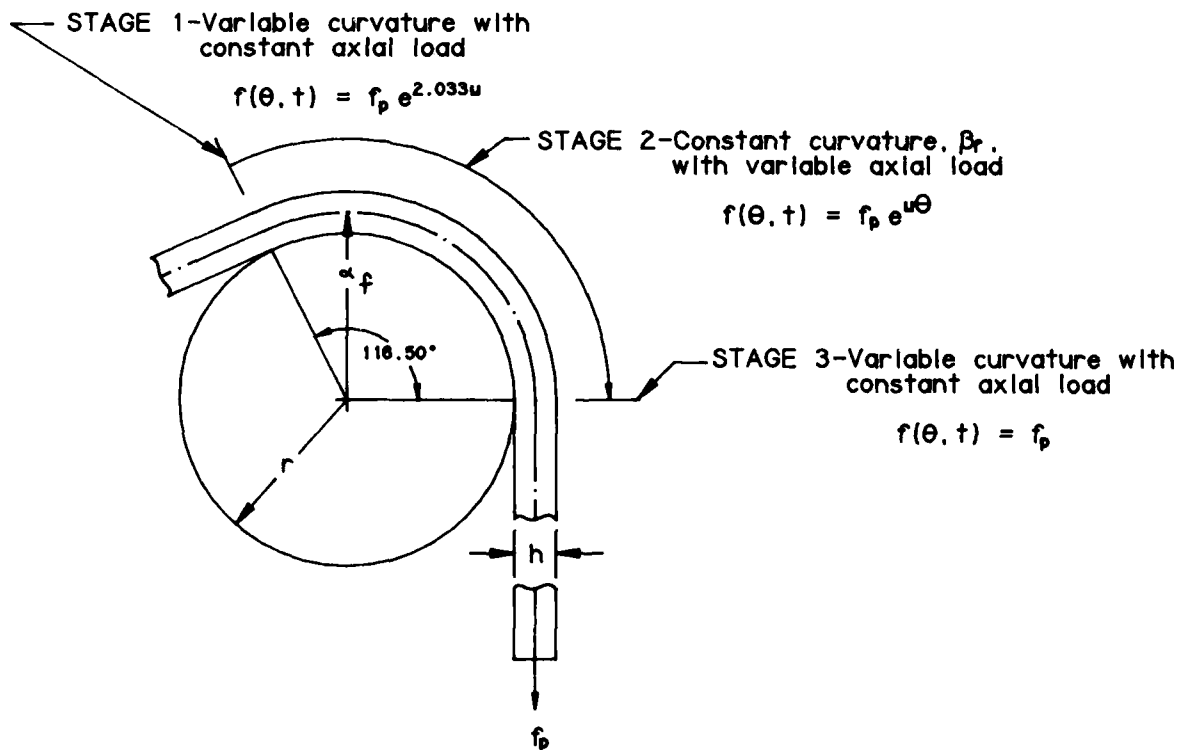
- (1) the flexible adherend conforms to the geometry of the roller throughout the peel process,
- (2) the adherend behaves as an elastic-plastic material with linear strain hardening (kinematic),
- (3) the strains are a linear function of the displacements (i.e., small displacement theory),
- (4) the strain distribution through the adherend thickness is always linear, and
- (5) the peel load that pulls the adherend around the roller acts in a manner similar to a flat belt drive problem, specifically, the force will vary exponentially along the surface of the roller [7].

$$f(\theta, t) = f_p e^{\mu\theta} \quad (1)$$

In the ASTM D3167 method, the flexible adherend is in contact with the roller for approximately 116.5 degrees (2.033 radians) as shown in Figure 3. The work required to deform the flexible adherend to the geometry of the roller can be divided into three stages:



(a) CURRENT FLOATING ROLLER TEST FIXTURE



(b) DEFORMATION STAGES OF ADHEREND

FIGURE 3 - GEOMETRY OF FLEXIBLE ADHEREND DEFORMATION DURING ASTM D3167 TEST

(1) the work to initially deform the adherend from zero to the curvature of the roller,

(2) the work to deform the adherend as it translates around the roller, and

(3) the work to straighten the adherend from the curvature of the roller to zero curvature.

The sum of the work from each stage gives the total work required to deform the flexible adherend.

In the first deformation stage, it is assumed that the bending deformation occurs instantaneously. The curvature of the flexible adherend varies from zero curvature to the maximum curvature, β_f , while the axial load remains constant.

$$\beta_f = \frac{1}{(r+h/2)} = 1/\alpha_f \quad (2)$$

The strains resulting from a constant axial load,

$$f(\theta, t) = f_p e^{2.033\mu} \quad (\text{where } \theta = 2.033 \text{ rad}) \quad (3)$$

are added to the strains produced from the bending load. Depending upon the thickness of the flexible adherend, the material may or may not undergo plastic deformation in the first stage.

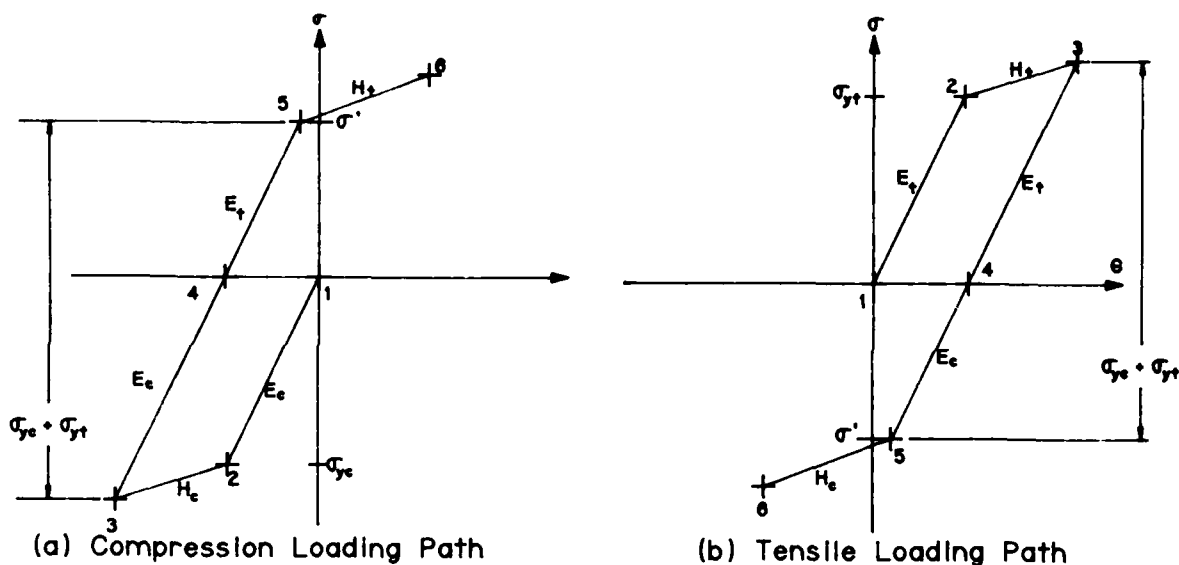
In the second deformation stage, the curvature of the adherend remains constant and the axial load is assumed to increase exponentially as the adherend translates along the surface of the roller (from assumption 5).

$$f(\theta, t) = f_p e^{\mu\theta} \quad (4)$$

As the angle θ decreases from 116.5° to 0° (2.033 to 0 radians), the axial load increases until it is equal to the peel force applied to the system. This force adds a tensile strain. Note that if the flexible adherend had been plastically deformed in the initial bending, the analysis must account for the change in

the loading path on the stress-strain curve. This tensile strain will cause the portion of the flexible adherend that was yielded in compression to unload along a path different from the initial loading path.

The change in loading paths is similar to the hysteresis effect of a magnetic material. For a typical position through the thickness of the adherend that undergoes plastic deformation, the change in the loading path will appear similar to that of Figure 4. When the adherend is initially loaded, the



- 1-2 Elastic loading
- 2-3 Plastic loading
- 3-4 Elastic unloading after plastic deformation
- 4-5 Elastic reloading after plastic deformation
- 5-6 Plastic reloading after plastic deformation

Figure 4. Loading Path for a Typical Point Undergoing Plastic Deformation in the Adherend.

adherend material will follow the path from point 1 to point 2 until it reaches the yield strength. After yielding the material will follow the path from point 2 to point 3 as the loading increases. Once the loading has reached the maximum value at point 3, upon unloading the material will follow the

path from point 3 to point 4. If the adherend is reloaded in the opposite direction, the material will continue along the elastic reloading path from point 4 to point 5. In the event that the reyielding stress, σ' , is exceeded, the material will proceed along the path from point 5 to point 6 for increased loading. One should remain aware of the fact that the strains vary linearly through the cross-section of the adherend. Thus, each point through the thickness of the adherend that is deformed plastically will have a unique loading/unloading/reloading path. Note that this analysis did account for the variation in the compressive and tensile material properties as shown in Figure 4 [8].

Before the second stage of the adherend deformation, only the unloading/reloading paths for the portion of the adherend yielded in compression requires computation. The increasing axial force in the second stage continues to load the portion of the adherend in tension, but unloads the portion of the adherend in compression. After the second deformation stage, however, the unloading/reloading paths for the portion of the adherend yielded in tension will require computation since the adherend will be subject to a reverse loading during the third stage of deformation.

In the third stage of deformation, it is assumed that the adherend straightens instantaneously. The axial load remains constant,

$$f(\theta, t) = f_p \quad (\text{where } \theta = 0 \text{ rad}) \quad (5)$$

while the curvature varies from the maximum curvature, β_f , to zero curvature. The bending strain is calculated as a function of the curvature and the axial strain is constant. In this third stage, the adherend is loaded in the reverse direction in comparison to the previous loadings in the first stage and second stage. Therefore, each position through the thickness of the adherend that was previously yielded in compression or tension will follow a unique unloading/reloading path as was

described earlier. The portion of the adherend not subject to plastic deformation will continue to follow the initial elastic loading paths. When calculating the work required to deform the adherend, one must be careful to account for the change in loading direction and the unique loading paths.

As mentioned previously, an energy approach is used to model the deformation of the adherend. For a Hookean material, the work per unit length is expressed as a function of the stress and the strain of the adherend as it deforms to the geometry of the roller [9].

$$W' = \int_A \sigma \epsilon \, dA \quad (6)$$

The stress and the strain can be expressed as a function of several known parameters, specifically the material properties, the applied peel force, and the geometry of deformation. Knowing the geometry of deformation, the engineering strain is computed at each position of the adherend throughout the peel process. The bending strain is calculated as a function of the curvature, β , of the midplane of the flexible adherend (Figure 5).

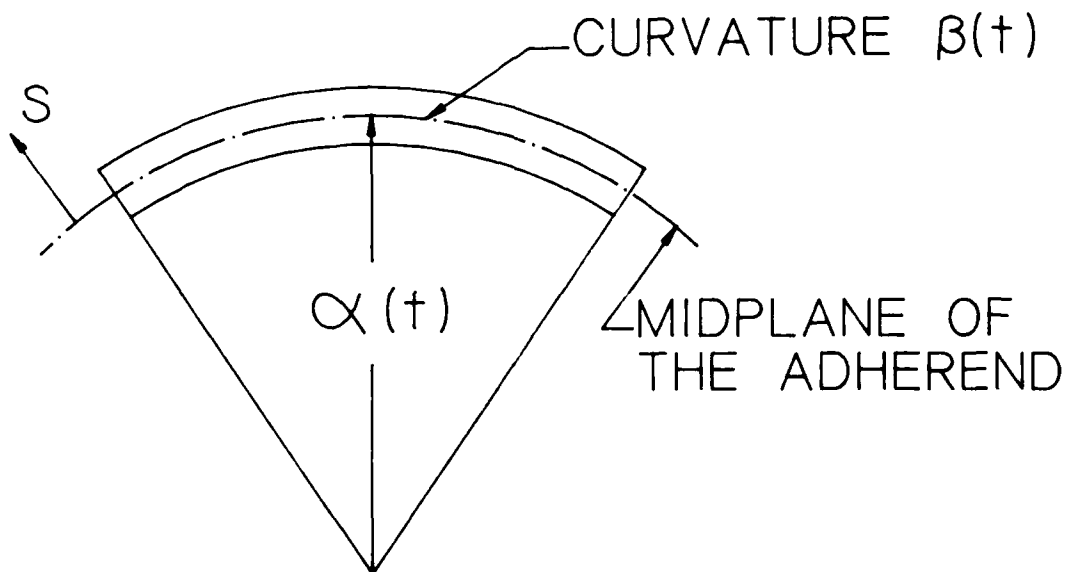


Figure 5. Geometry of Adherend.

Note that the curvature is simply the inverse of the radius of curvature, α , of the midplane.

$$\epsilon(s,t)_{\text{bending}} = \frac{(s + \frac{1}{\beta(t)})d\theta - \frac{1}{\beta(t)}d\theta}{\frac{1}{\beta(t)}d\theta} = \beta(t)s \quad (7)$$

The axial strains are expressed as a function of the axial load, $f(\theta, t)$, and an effective $EA(s, t)$.

$$\epsilon(s,t)_{\text{axial}} = \frac{f(\theta, t)}{EA(s, t)} \quad (8)$$

The effective $EA(s, t)$ will be constant as long as the adherend does not deform plastically. For inelastic deformation, however, the modulus of the material will vary through the thickness of the adherend. The effective $EA(s, t)$ is determined at any deformation state by integrating the variation in the modulus of the material over the area of the cross-section of the adherend.

$$EA(s, t) = \int_{-h/2}^{h/2} bE(s, t) ds \quad (9)$$

The total strain state is the sum of the axial and bending strains.

$$\begin{aligned} \epsilon(s, t) &= \epsilon(s, t)_{\text{bending}} + \epsilon(s, t)_{\text{axial}} \\ &= \beta(t)s + \frac{f(\theta, t)}{EA(s, t)} \end{aligned} \quad (10)$$

The stress state of the material is determined as a function of the strain. The stress is equivalent to

$$\sigma(s, t) = E\epsilon(s, t) \quad (11)$$

in the elastic region and

$$\sigma(s,t) = \sigma_0 \left(1 - \frac{H}{E}\right) + H\epsilon(s,t) \quad (12)$$

when the adherend deforms plastically. The work per unit length, W' , required to deform the flexible adherend is

$$W' = \int_{-h/2}^{h/2} \int_0^t b\sigma(s,t) \dot{\epsilon}(s,t) dt ds \quad (13)$$

where Equations 11 and 12 are substituted for the stress associated with elastic and inelastic deformation, respectively.

To solve for the work per unit length, the deformation process is broken into discrete time steps during the course of the peel test. It is also broken into discrete points through the thickness of the flexible adherend. The incremental work per unit length is calculated for each discrete time step by modifying Equation 13 so that the limits of integration are from t to $t+\Delta t$.

$$\Delta W' = \int_{-h/2}^{h/2} \int_t^{t+\Delta t} b\sigma(s,t) \dot{\epsilon}(s,t) dt ds \quad (14)$$

When the appropriate substitutions are made for the stress (Equations 11 and 12), Equation 14 can be expressed as

$$\Delta W' = \int_{-h/2}^{h/2} \int_t^{t+\Delta t} bE\epsilon(s,t) \dot{\epsilon}(s,t) dt ds \quad (15)$$

for elastic deformation and

$$\Delta W' = \int_{-h/2}^{h/2} \int_t^{t+\Delta t} b\left[\sigma_0\left(1 - \frac{H}{E}\right) + H\epsilon(s,t)\right] \dot{\epsilon}(s,t) dt ds \quad (16)$$

for inelastic deformation. If the strain rate, $\dot{\epsilon}(s,t)$ is assumed to occur at a constant rate over the incremental time step, Δt , Equations 15 and 16 can be integrated across the time step. Alternatively, Equations 15 and 16 are expressed as

$$\Delta W' = \int_{-h/2}^{h/2} bE (\epsilon(s, t+\Delta t)^2 - \epsilon(s, t)^2) ds \quad (17)$$

and

$$\Delta W' = \int_{-h/2}^{h/2} b \left\{ \sigma_0 \left(1 - \frac{H}{E} \right) [\epsilon(s, t+\Delta t) - \epsilon(s, t)] + H [\epsilon(s, t+\Delta t)^2 - \epsilon(s, t)^2] \right\} ds \quad (18)$$

respectively. As shown in these equations, the work per unit length is a function of the strain which, in turn, is a function of the curvature of the flexible adherend, the position s through the thickness of the adherend, and the axial force $f(\theta, t)$ as shown in Equation 10. Therefore, the required information is known and the incremental work per unit length can be calculated for each discrete time step. The total work per unit length is equal to the summation of the incremental values of the work per unit length for each discrete time step and is represented as

$$W' = \sum_{i=1}^n \Delta W_i \quad (19)$$

where n represents the number of time steps.

The analytical model was used to develop a computer program in order to accomplish the large number of stepwise calculations necessary to determine the work that is required to deform the flexible adherend. This model permits a quantitative determination of the percentage of the total work required to fail the adhesive in experimental tests and also allows direct comparison of variety of adhesives, regardless of test specimen construction, since the work to fail an adhesive can be distinguished from the work required to deform the flexible adherend.

SECTION 4

ANALYTICAL RESULTS FOR ADHEREND DEFORMATION

A study was performed to investigate the influence of several variables upon the work per unit length required to deform and pull the adherend around the roller of the test fixture. The material properties, adherend width, and radius of the roller were fixed. The variables subject to change were the applied peel force, coefficient of friction, and flexible adherend thickness. Two cases were analyzed. In one, the study described above was carried out for a flexible adherend of 6061-T6 aluminum alloy. In the second study the flexible adherend was 2024-T3 aluminum alloy. It was assumed that the aluminum alloy behaved as a linearly elastic-perfectly plastic material because of the similarities between the stress-strain curve of the 6061-T6 aluminum and the stress-strain curve of a linearly elastic-perfectly plastic material. Under this assumption the plastic moduli, H_C and H_t , are set equal to zero, and the plastic loading paths from point 2 to point 3 and from point 5 to point 6 in Figure 4 become horizontal lines.

For each case study, the adherend width and the radius of the roller were equal to 0.50 inch and 0.531 inch, respectively. The flexible adherend thickness was varied from 0.010 inch to 0.040 inch in 0.001 inch increments and the applied peel force ranged from 0 pounds to 100 pounds in 25 pound increments. In the analytical model, it was possible to choose any peel force, including zero. In reality, however, there exists a minimum peel force associated with deforming the adherend. The coefficient of friction was not of major concern since it only scales the magnitude of the peel force as it varies exponentially along the surface of the roller. Changes in the coefficient of friction would only affect the work per unit length calculated in the second stage of the deformation process and can be accounted for by a proportional change in the applied peel force. In other words, the variation in the coefficient of friction follows the same trend as the variation of the applied peel force.

In the case of the 6061-T6 alloy, the material properties are listed below [10].

Compressive elastic modulus	=	10.7×10^6 psi
Compressive plastic modulus	=	0 psi
Tensile elastic modulus	=	10.5×10^6 psi
Tensile plastic modulus	=	0 psi
Compressive yield strength	=	37,000 psi
Tensile yield strength	=	45,000 psi

The work per unit length generated using the analytical model is plotted as a function of the flexible adherend stiffness in Figure 6. In the figure, the peel force is the

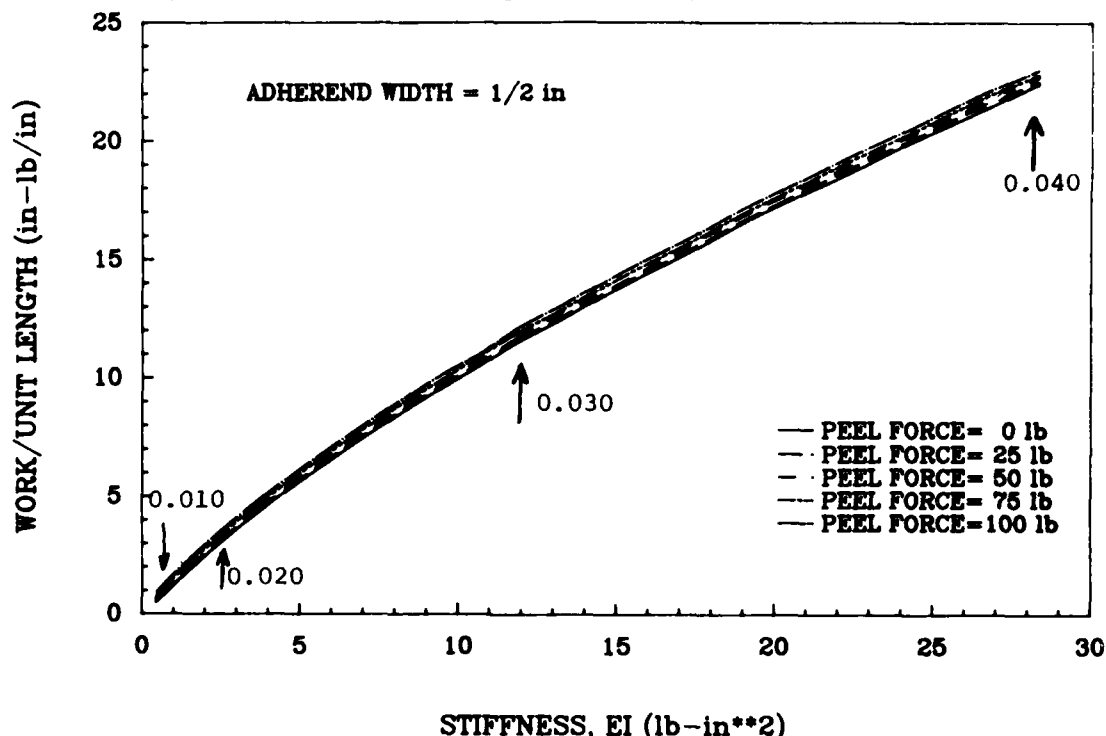


Figure 6. Analytical Results for the Flexible Adherend Deformation for 6061-T6 Aluminum.

applied peel force required to pull a test specimen through the test fixture during an experiment. The peel force was input into the model and can be selected based on past tests. If the selected peel force differs from the actual force, the percent error in the calculated work per unit length would be small, as shown in Figure 6. The variation in the thickness of the flexible adherend is expressed in units of stiffness along the

abscissa rather than units of length for a given width (ASTM specifies 0.5 inch wide specimens). Observe that the applied peel force does not significantly affect the work per unit length required to deform the flexible adherend. Changes in the flexible adherend thickness, however, have a substantial effect on the work per unit length to deform the adherend.

Furthermore, one can observe from Equations 17 and 18 that, for a specific thickness, the work per unit length is linearly proportional to the width of the adherend, thus changes in the width of the flexible adherend would also scale the curves vertically by a factor proportional to the width of the adherend. One should be cautioned that the stiffness scale for the peel curves in Figure 6 represent only changes in the flexible adherend thickness (the width is constant). Results generated with the analytical model for a different adherend width will correspond to a different set of peel curves.

In the second case, the same analysis was conducted for 2024-T3 aluminum alloy. These results are summarized in Figure 7. Again, it was assumed that the adherend behaved as a linearly elastic-perfectly plastic material. The material properties of the 2024-T3 aluminum alloy are listed below [10]:

Compressive elastic modulus	=	10.7×10^6	psi
Compressive plastic modulus	=	0	psi
Tensile elastic modulus	=	10.6×10^6	psi
Compressive plastic modulus	=	0	psi
Compressive yield strength	=	39,000	psi
Tensile yield strength	=	47,000	psi

The results for the 2024-T3 alloy are similar to the results generated for the 6061-T6 alloy. The small increase in the tensile and compressive yield strength of the 2024-T3 alloy, however, brings about a slight increase in the work per unit length needed to deform the adherend. This is evident when comparing the work per unit length required to deform an adherend made of both materials for a stiffness equal to 25 lb-in². When the peel force is equal to zero, the model predicts

that approximately 22 in-lb/in is required to deform the 6061-T6 adherend, whereas 23 in-lb/in is required to deform the 2024-T3 adherend. These differences are not apparent in the figures for lower stiffnesses.

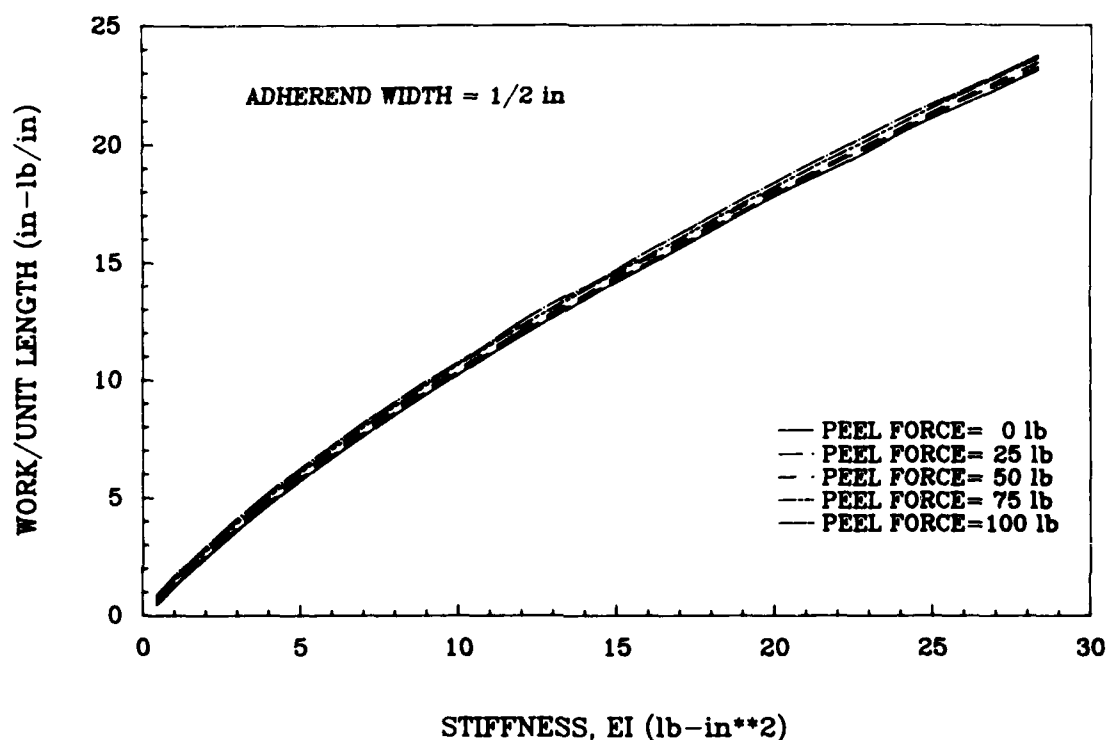


FIGURE 7—ANALYTICAL RESULTS FOR THE FLEXIBLE ADHEREND DEFORMATION FOR 2024-T3 ALUMINUM

SECTION 5
TEST FIXTURE MODIFICATION

The current Bell peel test fixture illustrated in D3167 performs well for adhesives that are strong relative to the adherend stiffness. As the ratio of peel strength to adherend stiffness decreases, however, problems arise because the fixture does not adequately constrain the peel specimen. These problems were discussed in some detail in Section 1. In view of the existing problems, UDRI has developed a modified test fixture that is able to adequately constrain the test specimen and avoid the problems encountered with the current Bell peel fixture. The UDRI fixture, illustrated in Figure 8, has the following advantages:

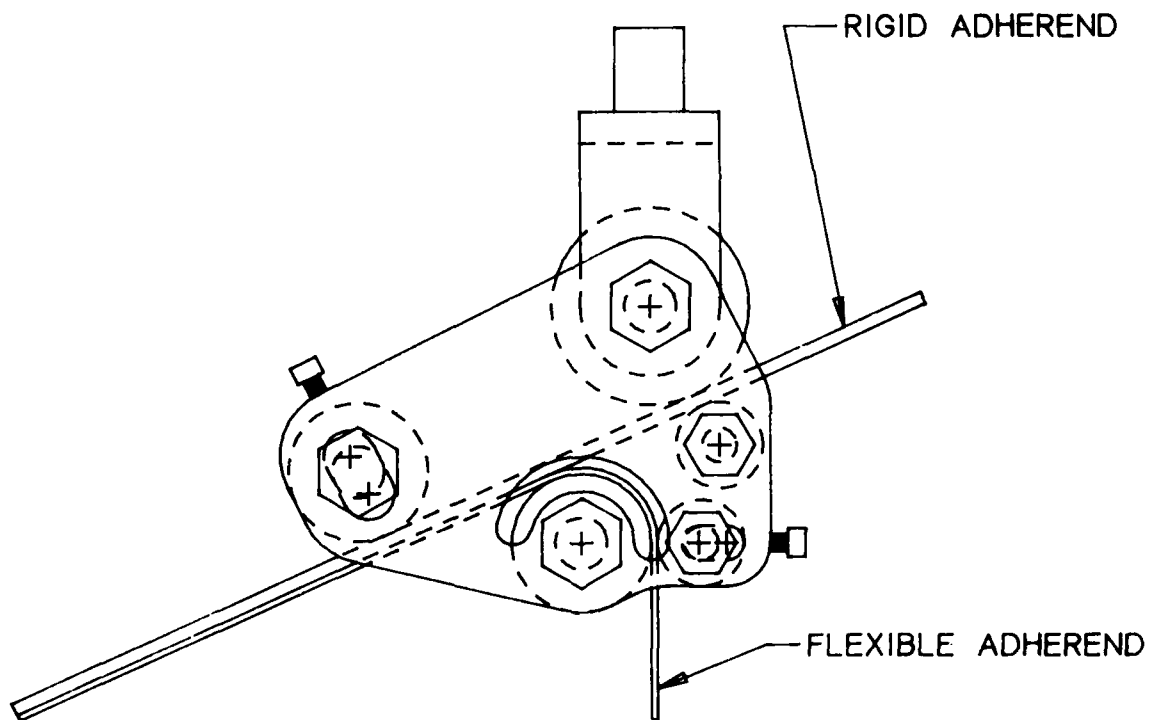


FIGURE 8 - UDRI TEST FIXTURE

- (1) one added roller prevents the free end of the test specimen from rising,
- (2) the angle of peel is held constant,
- (3) the adherend is forced to deform to the geometry of the roller (116.5° contact angle) by a second added roller,
- (4) consistent peel loads can be measured for any ratio of adhesive strength to adherend stiffness, and
- (5) the fixture is sensitive to small peel loads.

With the UDRI fixture, however, the test specimens had to be constructed 1-inch longer than the length specified in D3167 so that a full 6 inches of peel could be accomplished while the end of the specimen was still constrained by the added roller (Roller 1 as illustrated in Figure 16 of Appendix B).

Two experiments were conducted to compare the performance of the ASTM peel fixture and the UDRI fixture. One of the experiments involved bonding the flexible and rigid adherends together with intermittent segments of double-faced tape (Figure 9).

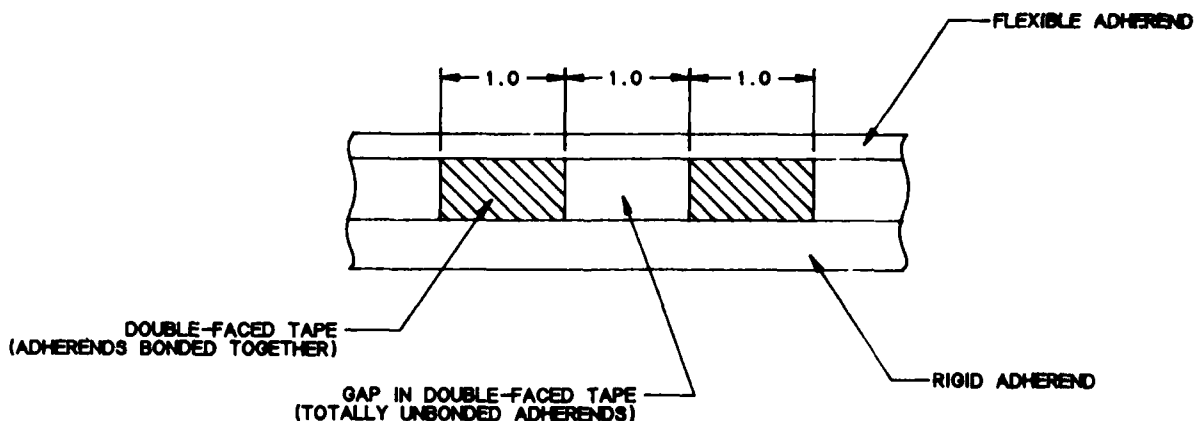


FIGURE 9 - SPECIMEN DESIGN WITH INTERMITTENT ADHEREND BONDING

The specimens were pulled through both fixtures at a rate of 6 inches per minute. It was expected that the plot of the peel load versus the distance peeled would look similar to Figure 10.

The peel load was measured for each case. The experimental results are presented in Figure 11.

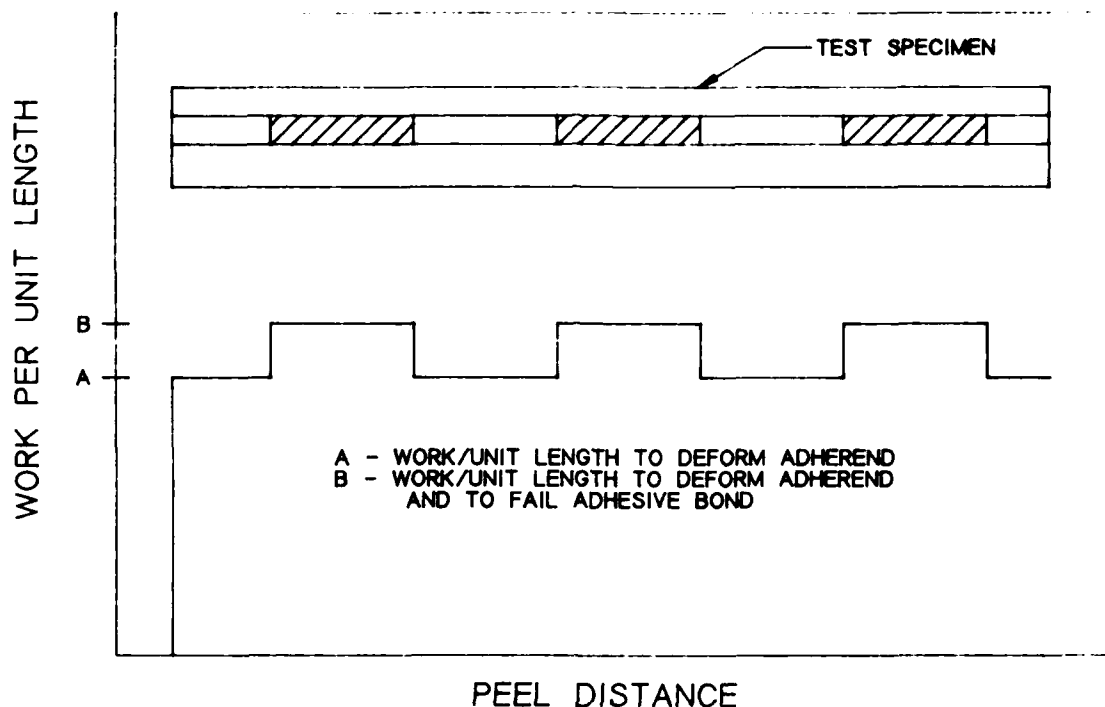


Figure 10. Expected Peel Results for Double-Faced Intermittent Tape.

The results obtained using the current ASTM test fixture are spiked and inconsistent and do not correspond to the locations of either taped or gap segments as they pass through the fixture. It can be seen that after failure of the first piece of tape the load decreases by about one-half. The second piece of tape is then loaded immediately before the 1-inch gap in the specimen has passed through the fixture. The specimen behaves in the manner illustrated in Figure 2b. It is impossible, from the measured data, to separate the load required to peel the adhesive from the load required to deform the adherend. The results using the UDRI fixture, however, correspond reasonably well to the expected pattern. The load required to peel the tape can be distinguished from the load required to deform the flexible adherend. Note that the loading is consistent and the measured results are sensitive. In this particular case, one

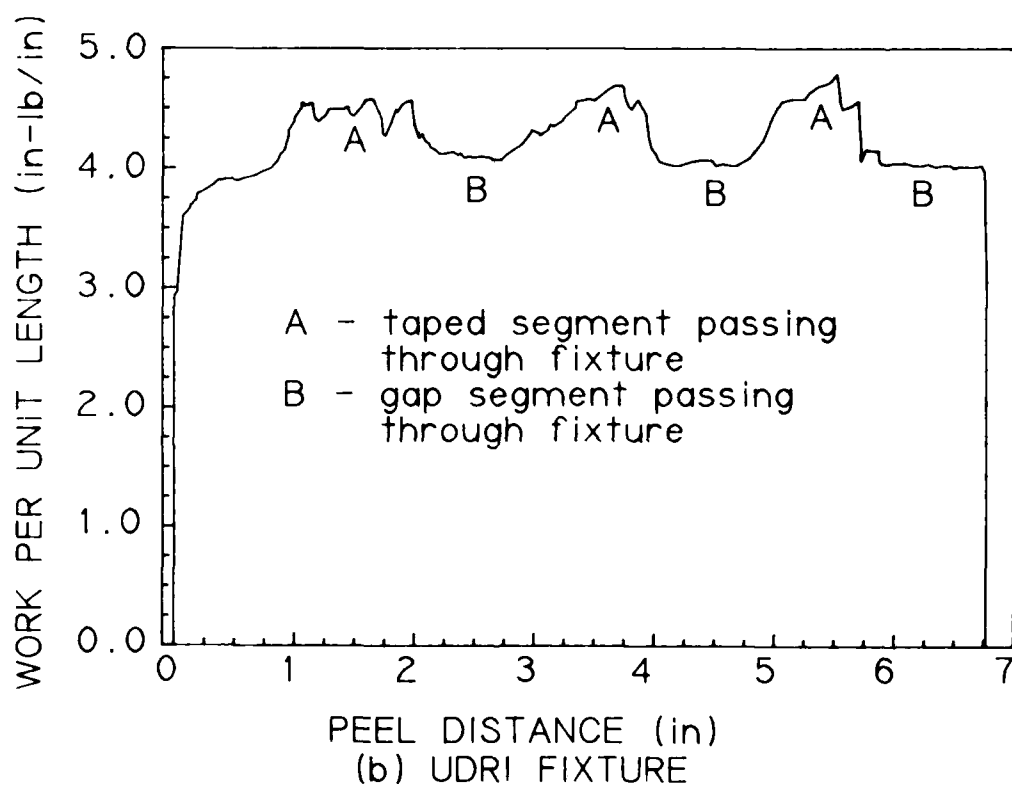
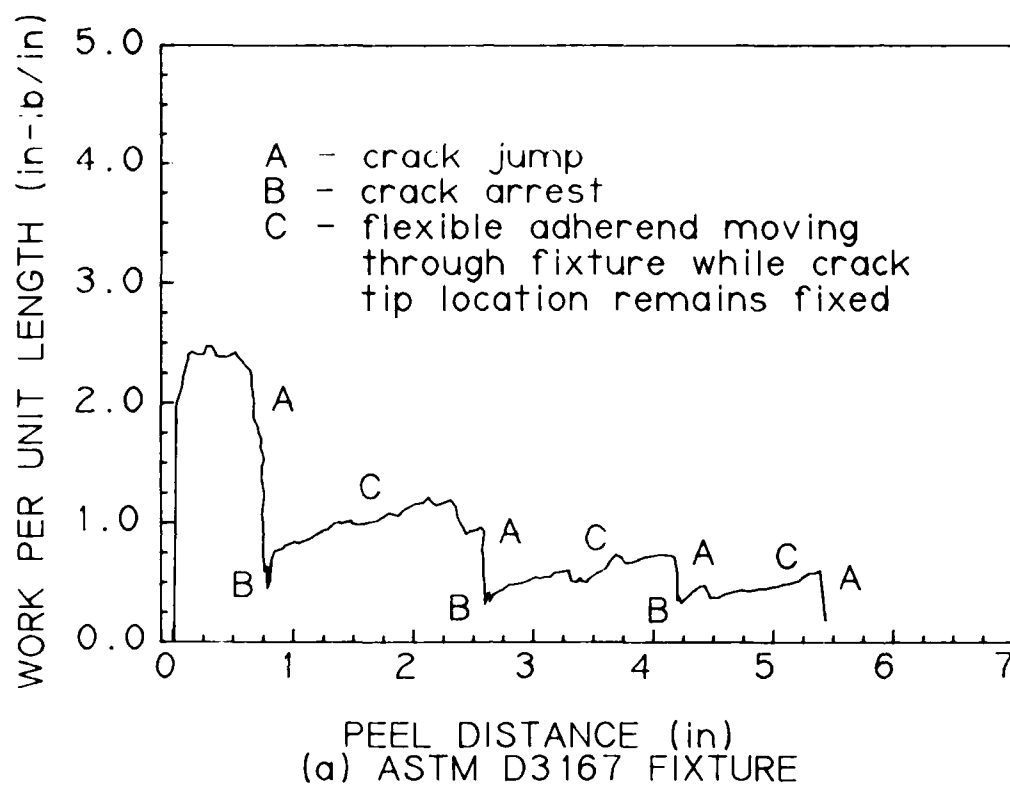


Figure 11. Peel Test Results with Intermittent Tape.

can conclude that a work per unit length of about 0.4 to 0.5 in-lb/in is required to peel the tape, with the remaining 4 in-lb/in being work per unit length to deform the flexible adherend.

In the second experiment, a comparison was made between the two fixtures for test specimens bonded with a weak adhesive. The specimens were fabricated in accordance with the ASTM specifications, with 2024-T3 aluminum alloy (0.020 inch flexible adherend thickness and 0.062 inch rigid adherend thickness) and Versilok® 204 adhesive. The peel tests were conducted at -67°F, at which temperature this adhesive has a relatively low peel strength. Several test specimens were pulled through both fixtures at a rate of 6 inches per minute. The results were recorded on an autograph machine, and the average work per unit length to fail the adhesive and to deform the adherend was calculated by collecting 1000 data points (during the peel test) with a computer having analog-to-digital conversion capabilities. The results for a typical specimen are illustrated in Figure 12. The average work per unit length to peel the specimens was 0.88 in-lb/in using the ASTM fixture and 7.08 in-lb/in using the UDRI fixture.

As shown in the figure, the crack jump/arrest behavior and the diminishing load pattern is apparent for the old fixture, whereas the new fixture produces a consistent load pattern. In Section 6 experimental results will be described which indicate that a work per unit length of 4.8 in-lb/in is required just to deform and pull a 0.020 inch thick adherend made from 2024-T3 aluminum alloy around the roller in the test fixture. The measured load when using the ASTM fixture, however, implies that a combined work per unit length of only 0.88 in-lb/in (Figure 12b) is required to both fail the adhesive and deform the adherend. In contrast, the measured loads when using the UDRI fixture show that a combined work per unit length of 7.08 in-lb/in (Figure 12a) is needed to fail the adhesive and to deform the adherend. Of this measured load, the analytical model predicts that 4.23 in-lb/in is required to deform the adherend,

®Trademark of the Lord Corporation.

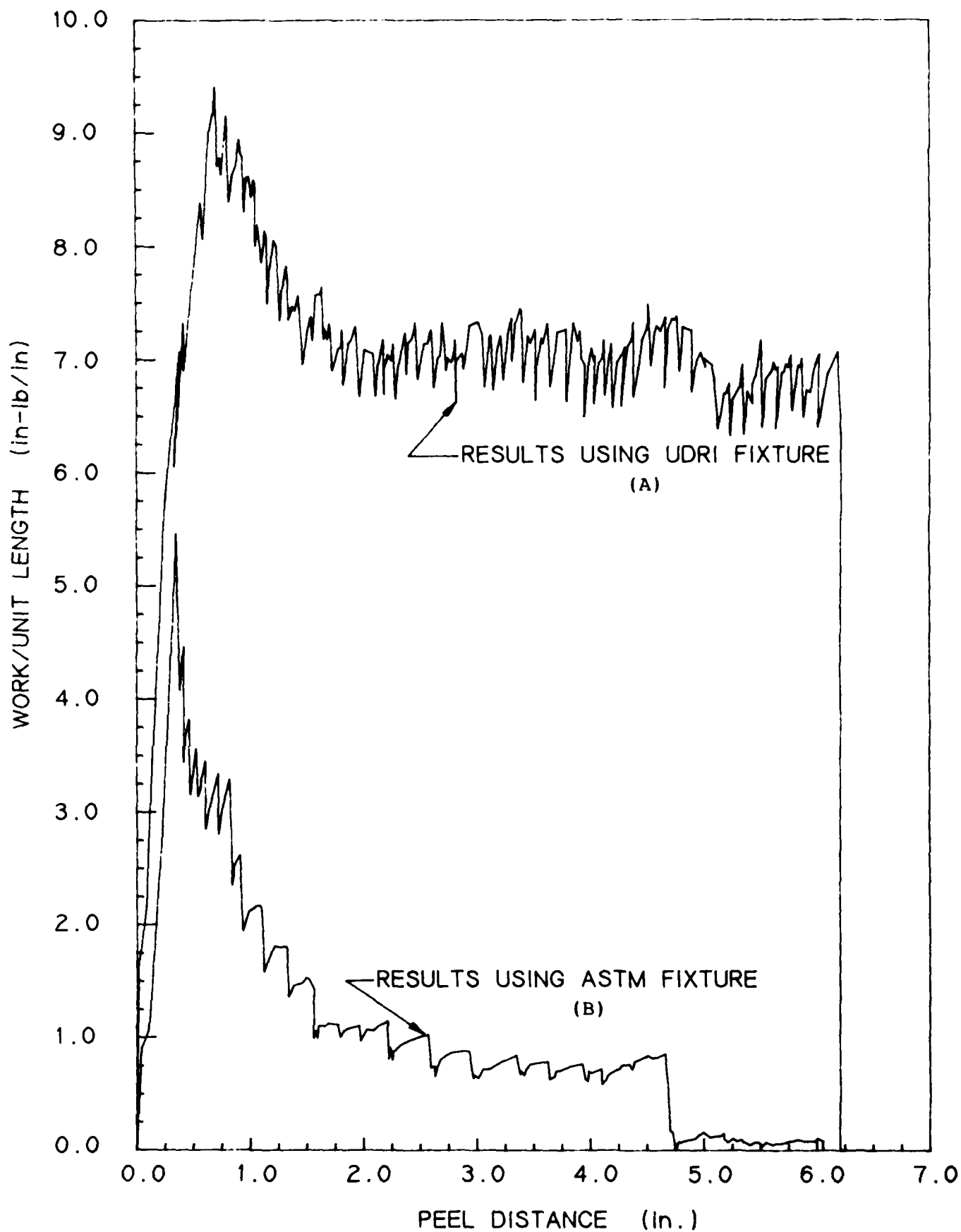


FIGURE 12 - COMPARISON OF MEASURED PEEL STRENGTHS OF A WEAK ADHESIVE AT -67 F

leaving the difference of 2.85 in-lb/in as the work per unit length (peel load) required to fail the adhesive. Note in this case that the experimentally measured work per unit length to deform the adherend around the roller in the test fixture (4.8 in-lb/in; described in Section 6), corresponds relatively closely to the value computed from the analytical model (4.23 in-lb/in).

Since at these low levels of peel load, the specimen fails in the manner illustrated in Figure 1b when the current ASTM fixture is used, it is impossible to apportion the measured load when using the ASTM fixture. Clearly, the data collected with the UDRI fixture is superior to that collected with the current ASTM fixture, particularly when used in conjunction with the analytical model.

In conclusion, the UDRI fixture is shown to be superior in performance compared to the ASTM fixture. The new fixture allows an analyst to collect consistent test results regardless of the adhesive strength or test conditions. Because the fixture adequately constrains the test specimen to the roller surface, the work per unit length required to deform the adherend can be computed analytically and can be distinguished from that required to fail the adhesive. A detailed drawing of the UDRI peel fixture and guidelines for its use can be found in Appendix B.

SECTION 6

EXPERIMENTAL RESULTS

Experiments were conducted with different flexible adherend materials and thicknesses to compare the results predicted by the analytical model with actual collected data. In one of the two experiments, the UDRI fixture was used to measure the work per unit length required only to deform the flexible adherend. In the second series of experiments, the adherends were bonded together with both a strong and weak adhesive. The specimens were pulled through both the UDRI fixture and the ASTM fixture to provide a comparison of the measured peel loads. An explanation of the experiments and the results is presented below.

In the first experiment, the flexible adherends consisted of two different materials (6061-T6 and 2024-T3 aluminum) which varied in thickness from 0.010 inch to 0.040 inch. Of the four specimens in each adherend group, three specimens of each group were approximately 1/2-inch wide, and the fourth was 1-inch wide. In order for these unbonded test specimens to translate through the UDRI fixture correctly, the rigid and flexible adherends were attached to each other at one end using masking tape. The tape acted like a rivet and prevented slipping between the rigid and flexible adherends. The specimens were pulled through the UDRI fixture at a rate of 6 inches/minute for a 6-inch distance. The work per unit length to deform the flexible adherend around the roller was recorded using an autograph machine, and the average work per unit length was calculated by sampling 1000 data points during the peel test using a computer with analog-to-digital conversion capabilities. The data points measured in the first and last inch of the test were excluded as specified in the current ASTM test procedure. The measured results are directly compared with results from the analytical model and are presented in Tables 1 and 2.

The experimental results for the 1/2-inch wide specimens were plotted on top of the curves illustrated in Figures 6 and 7

TABLE 1

COMPARISON OF ANALYTICAL AND EXPERIMENTAL PEEL LOADS
FOR VARIOUS ADHEREND STIFFNESSES¹

MATERIAL: 6061-T6 Bare

Thickness (in)	Width (in)	Stiffness (lb-in ²)	Experimentally Measured Force (lb)	W' to Deform Adherend (From model) (in-lb/in)
0.010	0.51	0.451	0.463	0.487
0.010	0.507	0.448	0.446	0.484
0.010	0.508	0.449	0.452	0.485
0.010	1.01	0.892	0.806	0.964
0.015	0.510	1.520	2.044	1.897
0.015	0.509	1.517	1.986	1.893
0.015	0.508	1.514	1.913	1.890
0.015	1.010	3.011	3.785	3.757
0.020	0.500	3.533	4.270	4.172
0.020	0.495	3.498	4.074	4.130
0.020	0.493	3.484	4.045	4.114
0.020	1.020	7.208	8.558	8.511
0.025	0.505	6.963	7.653	7.478
0.025	0.503	6.936	7.623	7.448
0.025	0.505	6.970	7.767	7.478
0.025	1.030	14.216	15.748	15.252
0.040	0.500	28.267	22.712	22.493
0.040	0.507	28.662	23.337	22.809
0.040	0.507	28.662	23.079	22.808
0.040	1.000	56.533	45.117	44.984

¹No actual peeling was occurring. The flexible adherend was simply being pulled through the UDRI peel test fixture.

TABLE 2

COMPARISON OF ANALYTICAL AND EXPERIMENTAL PEEL LOADS
FOR VARIOUS ADHEREND STIFFNESSES¹

MATERIAL: 2024-T3 Bare

Thickness (in)	Width (in)	Stiffness (lb-in ²)	Experimentally Measured Force (lb)	W' to Deform Adherend (From model) (in-lb/in)
0.010	0.510	0.451	0.491	0.466
0.010	0.509	0.450	0.458	0.465
0.010	0.508	0.449	0.458	0.464
0.010	1.01	0.890	0.899	0.923
0.015	0.508	1.514	1.828	1.886
0.015	0.510	1.520	1.990	1.893
0.015	0.508	1.514	1.870	1.886
0.015	1.01	3.011	3.510	3.749
0.020	0.503	3.555	4.796	4.258
0.020	0.503	3.555	4.687	4.257
0.020	0.508	3.590	4.901	4.300
0.020	1.000	7.066	9.376	8.464
0.025	0.500	6.901	7.933	7.572
0.025	0.503	6.942	7.889	7.615
0.025	0.503	6.942	7.979	7.615
0.025	0.907	12.518	14.752	13.733
0.032	0.503	14.559	15.906	13.929
0.032	0.503	14.559	16.084	13.929
0.032	0.503	17.559	15.958	13.929
0.032	1.020	29.524	33.680	28.251

¹No actual peeling was occurring. The flexible adherend was simply being pulled through the UDRI peel test fixture.

for these different adherend materials. The comparisons are presented in Figures 13 and 14. The curves correspond to the work per unit length generated by the analytical model for a range of peel forces and adherend stiffnesses, whereas the circles represent the experimentally measured work per unit length required to deform an adherend of a specific stiffness. Recall that the analytical results were generated using the assumption that the materials behaved as a linearly elastic-perfectly plastic material. If the width of a specimen in Tables 1 and 2 was not within 5% of the specified width (1/2 inch), the experimental result was not plotted in light of the fact that these experimental results would correspond to a different set of curves.

The results generated using the analytical model are shown to agree with the experimental data. Typically, the analytical results are slightly lower than the experimental results, especially for the thicker adherends. This difference can be attributed to the assumption of small displacement theory. In the development of the Green's strain approximation [6], the strains are a function of both linear and nonlinear terms of the displacement. For small displacement theory, however, the nonlinear terms are neglected, which implies that the strain approximation is a linear function of the displacement (corresponds to assumption 3 in Section 3)[6]. Actually, the nonlinear terms of the Green's strain approximation have a noticeable effect on the analytical results when a material deforms plastically but, in these two cases, would not improve results significantly. The majority of the analytical results for both alloys are within 5% of the experimental results. In the remaining cases, all but two were within 13% and the two extreme cases were within 19%.

In the second experiment, the rigid and flexible 6061-T6 adherends were bonded together with Versilok® 204/17 adhesive (low peel strength at -67°F) and 3M 3564B/3559A adhesive (high peel strength at 72°F). Four unprimed panels of each adhesive were fabricated. Two panels were constructed with a 0.020 inch

®Trademark of the Lord Corporation.

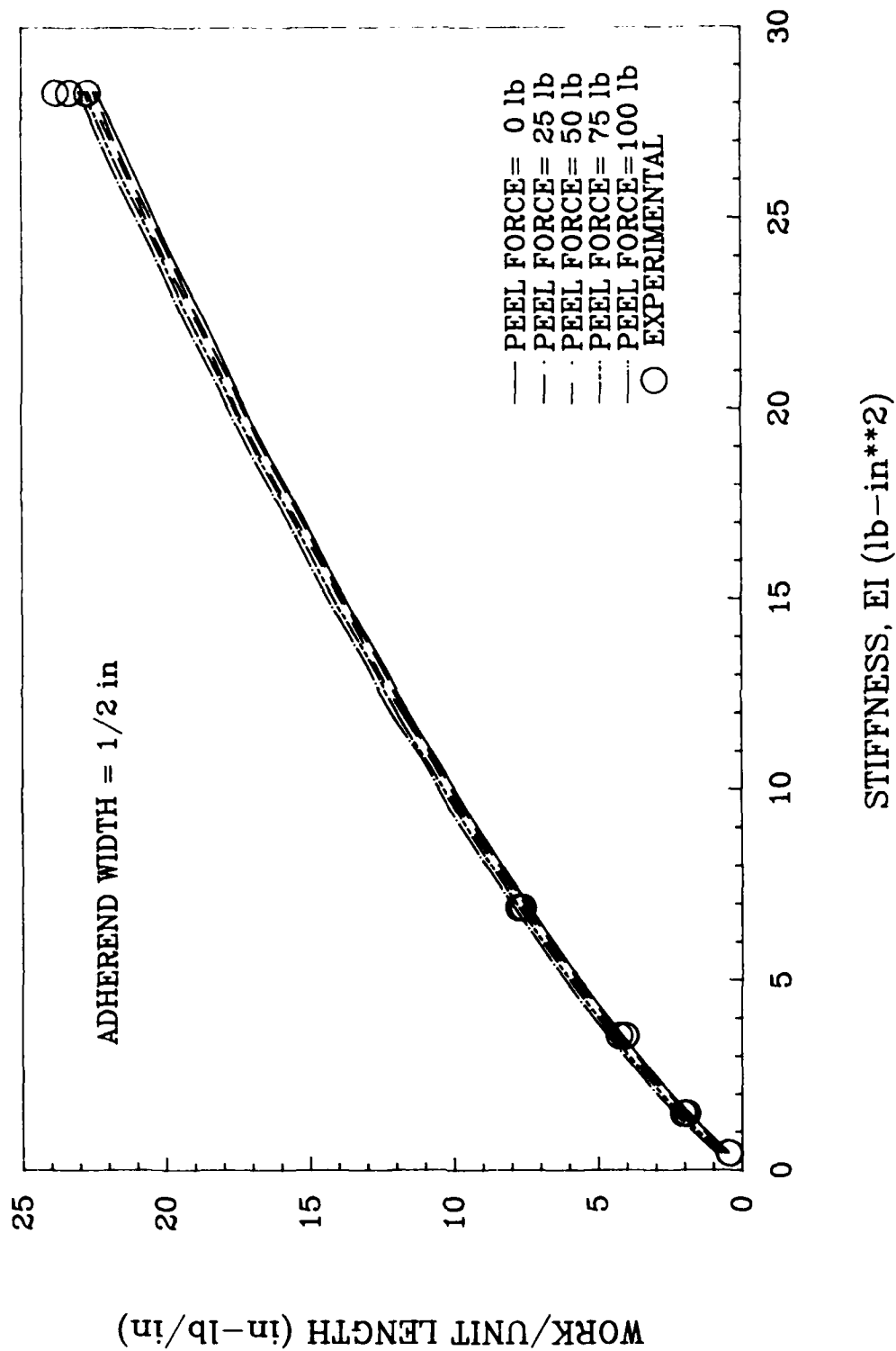


Figure 13. Comparison of Experimental Work Per Unit Length with Results from Analytical Model for 6061-T6.

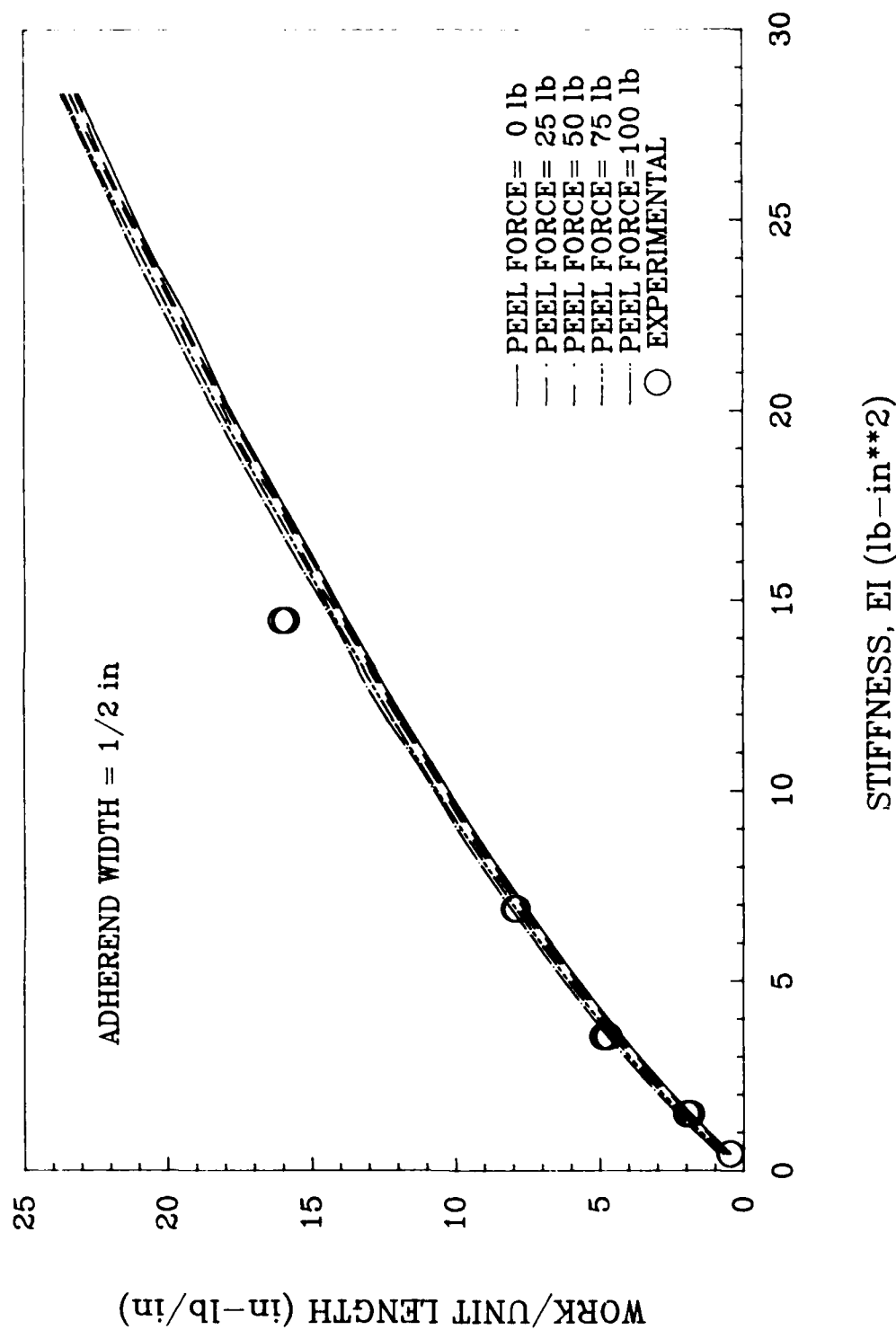


Figure 14. Comparison of Experimental Work Per Unit Length with Results from Analytical Model for 2024-T3.

flexible adherend and two panels were constructed with a 0.040 inch flexible adherend. One of the two panels in each group was bonded with the Versilok® adhesive and the other with the 3M adhesive. Each panel was cut into four test specimens which were 0.5 inch wide. Two of the specimens for each panel were tested using the ASTM fixture and the remaining two specimens were tested using the UDRI fixture. The specimens bonded with the Versilok® adhesive were tested at a temperature of -67°F to induce the low peel strength behavior. The specimens bonded with the 3M adhesive were tested at room temperature. Results for the specimens bonded with the Versilok® adhesive are presented in Table 3, while those for the 3M adhesive are summarized in Table 4.

In Table 3, which presents data for the low peel strength case, it can be observed that the measured values of the work per unit length required to peel the adhesive and to deform the adherend using the ASTM fixture are far below the experimental work per unit length required to deform only the adherend of the same thickness. When comparing the results for the specimens tested using the UDRI fixture with the experimental work per unit length required to deform the adherends, one can discriminate the portion of the total work required to fail the bond from that needed to deform the adherend. This discrimination cannot be made when using the ASTM fixture.

One would expect that if the analytical model for the work to deform the flexible adherend is accurate, the resulting work to fail the bond would be independent of the flexible adherend thickness (or stiffness). It is evident from the data in Table 3 that this is not the case. The peel strengths for the 0.020 and 0.040 inch adherends differ by approximately 1.4 in-lb/in. Part, and perhaps most, of this difference is due to the difference between the analytical and experimental results for the work to deform the flexible adherend (Figure 6). The remainder of this difference is attributable to the occurrence of different failure modes in specimens with different levels of flexible adherend thickness. All of the -67°F tests resulted in

®Trademark of the Lord Corporation.

TABLE 3

EXPERIMENTAL PEEL RESULTS FOR SPECIMENS BONDED WITH A
LOW PEEL STRENGTH ADHESIVE

Adherend Material: 6061-T6 Bare Aluminum
Adhesive: Versilok 204/17
Test Temperature: -67°F

<u>Speci- men No.</u>	<u>Thickness of Flexible Adherend (in)</u>	<u>Test Fixture</u>	<u>Experimental W' to Deform Adherend and Fail Adhesive Bond (in-lb/in)</u>	<u>Analytical W' to Deform the Adherend Only * (in-lb/in)</u>	<u>W' to Fail Adhesive Bond (Column 4- Column 5) (in-lb/in)</u>
1	0.020	ASTM	1.95	4.17	-
2	0.020	"	0.37	"	-
3	0.020	UDRI	5.03	"	0.86
4	0.020	"	5.06	"	0.89
1	0.040	ASTM	4.09	22.49	-
2	0.040	"	4.19	"	-
3	0.040	UDRI	24.78	"	2.29
4	0.040	"	24.84	"	2.35

* From Table 1 for 0.500 inch width.

TABLE 4

EXPERIMENTAL PEEL RESULTS FOR SPECIMENS BONDED WITH A
HIGH PEEL STRENGTH ADHESIVE

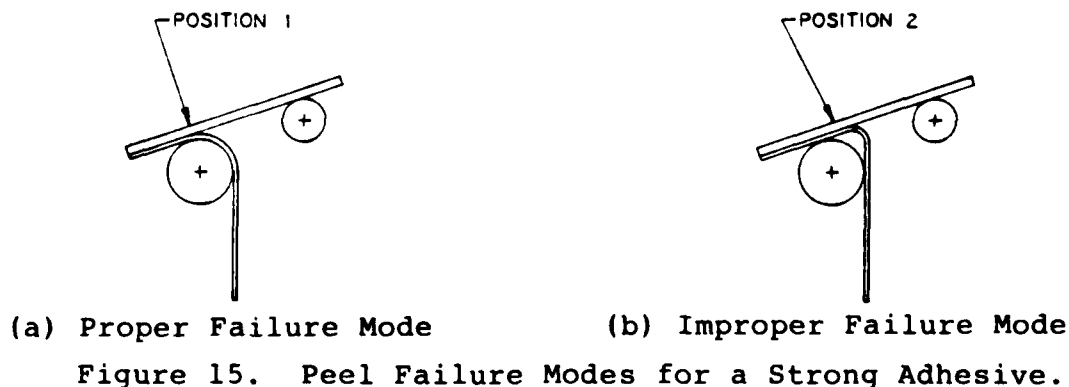
Adherend Material: 6061-T6 Bare Aluminum
Adhesive: 3M 3564B/3559A
Test Temperature: 72°F

Speci- men No.	Thickness of Flexible Adherend (in)	Test Fixture	Experimental W' to Deform Adherend and Fail Adhesive Bond (in-lb/in)	Analytical W' to Deform the Adherend Only* (in-lb/in)	W' to Fail Adhesive Bond (Column 4- Column 5) (in-lb/in)
1	0.020	ASTM	31.81	Avg: 4.17	27.64
2	0.020	"	33.65	"	29.48
3	0.020	UDRI	30.76	"	26.59
4	0.020	"	30.61	"	26.44
1	0.040	ASTM	42.22	Avg: 22.49	19.73
2	0.040	"	43.23	"	20.74
3	0.040	UDRI	43.30	"	20.81
4	0.040	"	42.23	"	19.74

* From Table 1 for 0.500 inch width.

adhesive failure between the unprimed flexible adherend and the adhesive layer. Thus, the work to fail the adhesive bond, listed in the last column of Table 3, is actually the work to fail the interface rather than the adhesive itself. Since the values for both the thin and thick adherend cases are low, it is felt that relatively minor differences in surface preparation could readily account for the difference in the results.

Table 4 contains the results for test specimens which were bonded with the 3M 3564B/3559A adhesive. For this case, in which the peel strengths are relatively high, the results using the UDRI fixture and the ASTM fixture were approximately the same for equivalent adherend thicknesses. This verifies that the design changes made on the test fixture do not influence the experimental results for adhesives with high peel strengths. Note that in this series of tests, one can discriminate between the work required to deform the adherend and the work needed to fail the adhesive bond for both test fixtures. Again there appears to be a discrepancy between the adhesive peel strength measured with the 0.020 inch adherend specimens and the 0.040 inch adherend specimens, even though the specimens were bonded with the same adhesive. As mentioned previously, one would expect the adhesive peel strengths (W' to fail the adhesive) to be equal regardless of the test specimen construction. This seeming inconsistency in the peel strength of the adhesive, however, is related to a difference in failure behavior between the thin and thick adherend specimens. For the case of the 0.020 inch adherend, the adhesive failure occurred at position 2, between the rollers, instead of at position 1 where the failure is supposed to occur (see Figure 15).



As a result of this failure behavior, the adherend deforms to a radius which is less than the radius of the roller (larger curvature) which, in turn, increases the strain state in the material. Increases in the strain will also increase the work per unit length required to deform the adherend. In contrast, the peel strengths for the specimens with 0.040 inch adherends were lower because the specimens failed in the proper mode during the test. Thus, this apparent discrepancy is not related to the model, but instead is the result of an imbalance in the ratio of the adhesive strength to the adherend stiffness. The indicated increase in the peel strength of the adhesive for the 0.020 inch adherend specimens is actually a result of the additional work per unit length required to deform the flexible adherend to a radius less than the radius of the roller.

As a result of this experiment, it was discovered that an additional problem exists with the Floating Roller Peel Test. In contrast to the problems which exist for low strength adhesives, another extreme exists where the adhesive strength becomes dominant and also causes the failure mode to occur away from the roller but in the other direction than in the case of low strength adhesives. This obviously affects the angle at which the flexible adherend is peeled from the rigid adherend. Technically, as cited in D3167, a direct comparison of peel results can only be made when specimen construction, test conditions, and peel angles are identical. Therefore, future work needs to be directed to establish criteria to govern the ratio of the peel strength of an adhesive to the stiffness of the flexible adherend to avoid the problems at both extremes.

SECTION 7

CONCLUSIONS

As a result of this investigation, the following conclusions were reached:

1. An analytical model was developed that is able to discriminate the work per unit length required to deform the flexible adherend from the work per unit length needed to fail the adhesive. The model agreed with the experimental results for the two aluminum alloys that were tested. The majority of the analytical results were within 5% of the experimental results and all except two were within 13%. The two worst cases were still within 19%.

2. The analytical model was used to write a computer program which allows the analyst to calculate the work required to deform the flexible adherend in a well behaved Floating Roller Peel test. This, in turn, permits the work needed to fail the adhesive to be partitioned out of the total measured peel load.

3. As a result of the deficiencies of the current ASTM test fixture, the University of Dayton Research Institute designed a modified test fixture to eliminate the existing problems when peeling low strength adhesives. The UDRI fixture adequately constrains the test specimen so that consistent results can be measured regardless of test specimen construction and test conditions. The UDRI fixture provides the capability of measuring a meaningful peel strength for the low peel strength adhesives. Experimental data collected with the UDRI fixture proved to be superior to the current ASTM fixture.

4. While the principal thrust of the test fixture redesign effort in this investigation was to overcome undesirable failure modes with low peel strength adhesives, one of the experiments indicated that undesirable failure modes can also occur with high peel strength adhesives. It would appear that some balance between adhesive peel strength and adherend

stiffness must be maintained in order for a peel test to provide a consistent and known failure mode and meaningful test results.

SECTION 8

RECOMMENDATIONS

As a result of this investigation, the authors recommend further investigation in the following areas:

1. Criteria should be established to govern the ratio of adhesive peel strength to adherend stiffness in order to avoid the two extremes in failure mode reported in this investigation. This criteria could be related to some material property of the adhesive, hopefully, such as flatwise tension or lap shear strength. In any event, this criteria appears necessary to enforce a consistent and analyzable failure mode of the adhesive in the peel test fixture.

2. Case studies (as described in the first experiment of Section 6) should be conducted for adherend materials other than aluminum alloys. Additional experiments should be conducted for the unbonded specimens (no adhesive) made from the various materials. The analytical results should be compared with experimental data (in the same manner as Figures 13 and 14) to determine the accuracy of the analytical model for the different adherend materials. The selected materials should have well defined properties in the plastic region, specifically the inelastic portion of the stress-strain curve should be in agreement with the assumption of linear strain hardening. Additional studies could be conducted for unbonded specimens subjected to different testing temperatures to determine whether the temperature significantly influences the measured work per unit length required to deform the flexible adherend. If the tests are sensitive to temperature, the analytical model should be refined to include temperature effects.

3. A similar investigation could be conducted for the Climbing Drum Peel Test (ASTM D1781). The analytical model for the Climbing Drum Peel Test can be developed by simply deleting the second and third stages of the deformation process of the analytical model developed for the Floating Roller Peel Test.

These adjustments can be made in the computer program found in Appendix A by deleting the appropriate part of the code which corresponds to the second and third stages of the deformation. The peel strength of the adherend should be converted to units of torque instead of work per unit length. Experimental data should be generated to verify the applicability of the new model to the CDP test.

REFERENCES

1. ASTM D1781-76, "Standard Method for Climbing Drum Peel Test for Adhesives," October 1976.
2. ASTM D3167-65, "Standard Test Method for Floating Roller Peel Resistance of Adhesives," October 1976.
3. D. H. Kaible, "Theory and Analysis of Peel Adhesion: Mechanisms and Mechanics," Transactions of the Society of Rheology, III, 1959, pp. 161-180.
4. D. H. Kaible, "Theory and Analysis of Peel Adhesion: Bond Stresses and Distribution," Transactions of the Society of Rheology, IV, 1960, pp. 45-73.
5. J. J. Bikerman, The Science of Adhesive Joints, Orlando: Academic Press, 1961, pp. 182-192.
6. Lawrence E. Malvern, Introduction to the Mechanics of a Continuous Medium, 1st ed., New Jersey: Prentice Hall, Inc., 1969, pp. 5, 154-161, 270.
7. Joseph E. Shigley, Mechanical Engineering Design, 4th ed., New York: McGraw-Hill Book Company, 1977, pp. 758-759.
8. Ferdinand P. Beer and E. Russell Johnston, Jr., Mechanics of Materials, 1st ed., New York: McGraw-Hill, Inc., 1981, pp. 184-192.
9. J. N. Reddy, Energy and Variational Method in Applied Mechanics, 1st ed., New York: John Wiley & Sons, Inc., 1984, pp. 90-95.
10. Military Standardization Handbook, "Metallic Materials and Elements for Aerospace Vehicles," MIL-HDBK-5D, Vol. 2, 1 June 1983, pp. 3-222, 3-234 and 3-72, 3-82.
11. Earl W. Swokowski, Calculus with Analytic Geometry, 2nd ed., Massachusetts: Prindle, Weber & Schmidt, 1979, pp. 259-260.

NOMENCLATURE

t	Time
Δt	Incremental time step
h	Thickness of the flexible adherend
b	Width of the flexible adherend
s	Through the thickness coordinate axis, referenced at the midplane of the flexible adherend
$\epsilon(s, t)$	Strain at position s through the thickness of the flexible adherend for the deformation state at time t
$\sigma(s, t)$	Stress at position s through the thickness of the flexible adherend for the deformation state at time t
σ_{ot}	Initial tensile yield strength of the flexible adherend
σ_{oc}	Initial compressive yield strength of the flexible adherend
σ'	Reyielding strength of the flexible adherend
E_c	Compressive elastic modulus of the flexible adherend
H_c	Compressive plastic modulus of the flexible adherend
E_t	Tensile elastic modulus of the flexible adherend
H_t	Tensile plastic modulus of the flexible adherend
r	Radius of the roller of the test fixture
θ	Angle of contact between the flexible adherend and the roller
μ	Coefficient of friction between the flexible adherend and the roller
$EA(s, t)$	Effective EA when adherend begins to plastically deform
$\alpha(t)$	Radius of curvature of the midplane of the flexible adherend as it conforms to the geometry of the roller
$\beta(t)$	Curvature of the midplane of the flexible adherend
f_p	Applied peel force (measured experimentally) to pull the specimen through the test fixture
$f(\theta, t)$	Peel force at angle of contact θ and deformation state at time t
W'	Work per unit length to deform the flexible adherend
$\Delta W'$	Incremental work per unit length to deform the flexible adherend

A	Cross-sectional area of the flexible adherend
β_f	Maximum curvature of the midplane of the flexible adherend when deformed to the geometry of the roller
$\dot{\epsilon}(s,t)$	Strain rate
α_f	Minimum radius of curvature of the midplane of the flexible adherend when deformed to the geometry of the roller

APPENDIX A

COMPUTER ANALYSIS OF PEEL PROCESS

A computer program is used to carry out the large number of iterations. The thickness of the flexible adherend is divided into 500 finite increments, and deformation process is divided into a total of 300 time steps; each stage of the deformation is broken into 100 time steps. Therefore, the incremental work per unit length is calculated 300 times at 500 different positions through the thickness of the adherend using Equations 17 and 18 in Section 2. For computers with larger storage capacities, the number of iterations can be increased by changing the appropriate variables in the computer code. The accuracy of the results, however, will not improve significantly. The trapezoidal rule is used to integrate the equations numerically [11]. The program is able to approximate the work per unit length required to deform the adherend and the work per unit length needed to fail the adhesive.

The program is easy to use and only requires the user to create a data file. The input parameters are the material properties, the dimensions of the flexible adherend, the radius of the roller, and the measured peel load from the experiment. The data file must include the following parameters in the respective order (all positive real numbers):

- (1) Radius of the roller
- (2) Compressive yield strength of the flexible adherend
- (3) Tensile yield strength of the flexible adherend
- (4) Compressive elastic modulus of the adherend
- (5) Tensile elastic modulus of the adherend
- (6) Compressive plastic modulus of the adherend
- (7) Tensile plastic modulus of the adherend.

The parameters are to be entered in a row with a comma separating each parameter. The program will prompt the user to input the width and thickness of the flexible adherend and the measured experimental peel force. The units for all the

parameters must be compatible and should be expressed in inches and pounds for the English measurement system.

The output data can be displayed in a data file or on the screen by setting the parameter NOUT equal to 2 or 6, respectively. The output will list all input parameters, the work per unit length required to deform the adherend, and the work per unit length to fail the adhesive. It will also list the percentage of the total work required to deform the adherend and to fail the adhesive. The peel strength of the adhesive, as defined in ASTM D3167, is found by dividing the work per unit length to fail the adhesive by the width of the adherend.

The computer code is written using the VAX/VMS FORTRAN language, a subset of the ANSI FORTRAN 77 standard. The compiler version is 4.1.

PROGRAM FEEL

PARAMETER CONTACT ANGLE = 116.5, NG=505, NY=105,
 NI=105, DEG TO RAD = 0.1745)

DEFINITION OF VARIABLES

R = RADIUS OF ROLLER
 A = CROSS-SECTIONAL AREA OF ADHEREND
 B = WIDTH OF ADHEREND
 H = THICKNESS OF ADHEREND
 EC = ELASTIC MODULUS OF ADHEREND (COMPRESSION)
 ET = ELASTIC MODULUS OF ADHEREND (TENSILE)
 HC = PLASTIC MODULUS OF ADHEREND (COMPRESSION)
 HT = PLASTIC MODULUS OF ADHEREND (TENSILE)
 SIGMAT = YIELD STRENGTH OF ADHEREND (TENSILE)
 SIGMAC = YIELD STRENGTH OF ADHEREND (COMPRESSION)
 EPSILONT = INITIAL YIELD STRAIN (TENSILE)
 EPSILONC = INITIAL YIELD STRAIN (COMPRESSION)
 FRICTION = COEFFICIENT OF FRICTION BETWEEN ADHEREND AND ROLLER
 ARCLEN = ARC LENGTH OF MID-PLANE OF ADHEREND WHEN IN CONTACT WITH ROLLER
 ALPHA = RADIUS OF CURVATURE OF MID-PLANE OF ADHEREND
 S = DISTANCE FROM MID-PLANE OF ADHEREND TO POSITION THROUGH THICKNESS OF ADHEREND
 DS = INCREMENTAL DISTANCE THROUGH THICKNESS OF ADHEREND
 NS = NUMBER OF INCREMENTAL DISTANCES THROUGH THICKNESS OF ADHEREND
 BETA = CURVATURE OF MID-PLANE OF ADHEREND
 DBETA = INCREMENTAL CURVATURE
 NBETA = NUMBER OF INCREMENTAL CURVATURES
 THETAX = VARIABLE ANGLE IN WHICH ADHEREND CONTACTS ROLLER (RADIAN)
 THETAF = TOTAL ANGLE OF CONTACT (RADIAN)
 DTHETA = INCREMENTAL ANGLE
 NTHETA = NUMBER OF INCREMENTAL ANGLES
 TESTSTRAIN = TEST CURRENT STRAIN OF YIELDING
 CRESSTRAIN = RESIDUAL STRAIN FOR PORTION OF ADHEREND YIELDED IN COMPRESSION
 TRESSTRAIN = RESIDUAL STRAIN FOR PORTION OF ADHEREND YIELDED IN TENSION
 RESSTRAIN = COMBINED RESIDUAL STRAIN (CRESSTRAIN AND TRESSTRAIN)
 EPSYT = NEW YIELD STRAIN AFTER PLASTIC DEFORMATION (TENSILE)
 EPSYC = NEW YIELD STRAIN AFTER PLASTIC DEFORMATION (COMPRESSIVE)
 BC = Y-INTERCEPT OF COMPRESSION UNLOADING CURVE AFTER PLASTIC DEFORMATION AT POSITION S(I)
 BT = Y-INTERCEPT OF TENSION UNLOADING CURVE AFTER PLASTIC DEFORMATION AT POSITION S(I)
 BCP = Y-INTERCEPT OF ELASTIC RELOADING CURVE AT POSITION S(I) (COMPRESSIVE)
 BTP = Y-INTERCEPT OF ELASTIC RELOADING CURVE AT POSITION S(I) (TENSILE)
 BCPP = Y-INTERCEPT OF PLASTIC RELOADING CURVE AT POSITION S(I) (COMPRESSIVE)
 BTPP = Y-INTERCEPT OF PLASTIC RELOADING CURVE AT POSITION S(I) (TENSILE)


```

SIGMAXC = MAXIMUM STRESS OF POSITION S(I) (COMPRESSION)
SIGMAXT = MAXIMUM STRESS OF POSITION S(I) (TENSILE)
SIGRYC = RE-YIELD STRESS AFTER STRAIN HARDENING
          (COMPRESSION LOADING PATH)
SIGRYT = RE-YIELD STRESS AFTER STRAIN HARDENING
          (TENSILE LOADING PATH)
EA = EFFECTIVE E*A
DU = INCREMENTAL STRAIN ENERGY DENSITY
EPS1 = STRAIN AT POSITION S(I) FOR CURVATURE BETA(J).
       STRAIN IS CALCULATED FROM ZERO TO FINAL
       CURVATURE (1/ALPHA).
EPS2 = STRAIN AT POSITION S(I) FOR CONTACT ANGLE
       THETAX(J). STRAIN IS CALCULATED FROM 116.5
       TO 0.0 DEGREES.
EPS3 = STRAIN AT POSITION S(I) FOR CURVATURE BETA(J).
       STRAIN IS CALCULATED FROM FINAL CURVATURE
       (1/ALPHA) TO ZERO CURVATURE.
U1 = INCREMENTAL STRAIN ENERGY DENSITY OF ADHEREND AS
      IT DEFORMS FROM CURVATURE BETA(J) TO BETA(J+1)
U2 = INCREMENTAL STRAIN ENERGY DENSITY OF ADHEREND AS
      IT TRANSLATES AROUND ROLLER FROM THETAX(J) TO
      THETAX(J+1)
U3 = INCREMENTAL STRAIN ENERGY DENSITY OF ADHEREND AS
      IT DEFORMS FROM CURVATURE BETA(J) TO BETA(J-1)
W1 = WORK/UNIT LENGTH TO BEND ADHEREND
W2 = WORK/UNIT LENGTH WHEN ADHEREND TRANSLATES
      AROUND ROLLER
W3 = WORK/UNIT LENGTH TO STRAIGHTEN ADHEREND
WORK = TOTAL WORK/UNIT LENGTH TO DEFORM ADHEREND
WORKADS = WORK/UNIT LENGTH TO FAIL ADHESIVE
PERADH = PERCENTAGE OF THE TOTAL WORK/UNIT LENGTH TO
        DEFORM THE FLEXIBLE ADHEREND
PERADS = PERCENTAGE OF THE TOTAL WORK/UNIT LENGTH TO
        TO FAIL THE ADHESIVE
ASTM = PEEL STRENGTH OF THE ADHESIVE AS DEFINED IN THE
        ASTM D3167. EQUAL TO THE WORK/UNIT LENGTH TO
        FAIL ADHESIVE DIVIDED BY THE WIDTH OF THE
        ADHEREND

```

```

*****
IMPLICIT DOUBLE PRECISION(A-H,O-Z)

```

```

DIMENSION EPS1(NX,NY),EP(NX),EA(NX),
#       DU(NX),S(NX),BETA(NY),F(N1),
#       EPS3(NX,NY),BCP(NX),BTP(NX),
#       EPSYT(NX),EPSYC(NX),EPS2(NX,NY),
#       CRESSTRAIN(NX),TRESSTRAIN(NX),
#       RESSTRAIN(NX),SIGMAXT(NX),THETAX(N1),
#       BC(NX),BT(NX),SIGMAXC(NX),
#       SIGRYC(NX),SIGRYT(NX),BCPP(NX),
#       BTPP(NX)

```

```

OPEN(1,FILE='PEEL.DAT',STATUS='OLD')
OPEN(2,FILE='PEEL.OUT',STATUS='NEW')

```

```

NDOUT=6

```

```

READ(1,*)R,SIGMAC,SIGMAT,EC,ET,HC,H1
WRITE(6,5)
5 FORMAT(/5X,'INPUT EXPERIMENTAL PEEL LOAD')
READ(5,*)FP
WRITE(6,6)

```

```

6 FORMAT(/5X, 'INPUT WIDTH OF SPECIMEN (INCHES)')
  READ(5,*)B
  WRITE(6,7)
7 FORMAT(/5X, 'INPUT THICKNESS OF SPECIMEN (INCHES)')
  READ(5,*)H

```

```

C
  WRITE(NDOUT,8)EC,HC,ET,HT,SIGMAT,SIGMAC,R,B,H,FP
8 FORMAT(/1X, '*****',
#      '*****',/26X, 'I N P U T',
#      ' D A T A',/1X, '*****',
#      '*****',
#      /5X, 'COMPRESSIVE ELASTIC MODULUS (psi) = ',E10.4,
#      /5X, 'COMPRESSIVE PLASTIC MODULUS (psi) = ',E10.4,
#      /5X, 'TENSILE ELASTIC MODULUS (psi) = ',E10.4,
#      /5X, 'TENSILE PLASTIC MODULUS (psi) = ',E10.4,
#      /5X, 'TENSILE YIELD STRENGTH (psi) = ',E10.4,
#      /5X, 'COMPRESSIVE YIELD STRENGTH (psi) = ',E10.4,
#      /5X, 'RADIUS OF ROLLER (in) = ',F6.4,
#      /5X, 'WIDTH OF SPECIMEN (in) = ',F6.4,
#      /5X, 'THICKNESS OF SPECIMEN (in) = ',F6.4,
#      /5X, 'EXPERIMENTAL PEEL LOAD (lbs) = ',F6.2)

```

```

FRICITION = .3
ARCLN = (CONTACT_ANGLE*DEG_TO_RAD)*(R+H/2.)
ALPHA = R+H/2.
DS = H/500.
NS = NINT(H/DS)
DBETA = (1./ALPHA)/100.
NBETA = NINT(1./(DBETA*ALPHA))
EPSILONT = SIGMAT/ET
EPSILONC = -SIGMAC/EC
W1 = 0.0
W2 = 0.0
W3 = 0.0
A = B*H
SI = -H/2.
FI = FP/(EXP(FRICITION*ARCLN*(1./ALPHA)))

```

```

C
C *****
C CALCULATE STRAINS FOR FIRST DEFORMATION STAGE OF
C THE FLEXIBLE ADHEREND
C *****

```

```

C
  DO 20 I=1,NBETA+1
    BETA(I) = (1./ALPHA)*(I-1)/NBETA
  DO 9 K=1,NS+1
    S(K) = SI+H*(K-1)/NS
    EP(K) = BETA(I)*S(K)
  9 CONTINUE

  CALL EAEFF1(EPSILONC, EPSILONT, HC, EC, ET, HT, B, DS, NS, EA, I, EP)

  DO 10 J=1,NS+1
    EPS1(J, I) = EP(J)+FI/EA(I)
  10 CONTINUE
  20 CONTINUE

```

```

C *****
C CALCULATE INCREMENTAL STRAIN ENERGY DENSITY FOR FIRST
C DEFORMATION STAGE OF FLEXIBLE ADHEREND
C *****

```

```

DO 70 J=1,NBETA

```

```

DO 60 J=1,NS+1
  TESTSTRAIN=EPS1(J, I+1)
  IF (TESTSTRAIN.GE. EPSILONC) GOTO 30
    DU(J)= (-SIGMAC*(1-HC/EC)+(HC/2.)*(EPS1(J, I+1)+
      EPS1(J, I)))*(EPS1(J, I+1)-EPS1(J, I))
    GOTO 60
  30 IF (TESTSTRAIN.GT. 0.0) GOTO 40
    DU(J)= (EC/2.)*(EPS1(J, I+1)**2.-EPS1(J, I)**2.)
    GOTO 60
  40 IF (TESTSTRAIN.GT. EPSILONL) GOTO 50
    DU(J)= (ET/2.)*(EPS1(J, I+1)**2.-EPS1(J, I)**2.)
    GOTO 60
  50 DU(J)= (SIGMAT*(1-HT/ET)+(HT/2.)*(EPS1(J, I+1)+
    EPS1(J, I)))*(EPS1(J, I+1)-EPS1(J, I))
  60 CONTINUE

  *****
  CALCULATE WORK/UNIT LENGTH FOR FIRST DEFORMATION STAGE
  OF THE FLEXIBLE ADHEREND
  *****

  U1=0.0
  CALL TRAPRULE(U1,DS,NS,DU)

  U1= U1*B
  W1= W1+U1
  70 CONTINUE

  THETA= CONTACT_ANGLE*DEG_TO_RAD
  DTHETA= THETA/100.
  NTHETA= NINT(THETA/DTHETA)

  *****
  CALCULATE UNLOADING/RELOADING STRESS-STRAIN PATHS FOR
  PORTION OF FLEXIBLE ADHEREND YIELDED IN COMPRESSION
  *****

DO 600 I=1,NS+1
  IF (EPS1(I,NBETA+1).LT. EPSILONC) THEN
    SIGMAXC(I) = -SIGMAC+(EPS1(I,NBETA+1)-EPSILONC)*HC
    SIGRYT(I) = SIGMAXC(I)+(SIGMAT+SIGMAC)
    BC(I) = SIGMAXC(I)-EC*EPS1(I,NBETA+1)
    CRESSTRAIN(I)= -BC(I)/EC
    BTP(I) = -CRESSTRAIN(I)*ET
    EPSYT(I) = (SIGRYT(I)-BTP(I))/ET
    BTPP(I) = SIGRYT(I)-HT*EPSYT(I)
  ELSE
    BC(I) = 0.0
    CRESSTRAIN(I)= 0.0
    BTP(I) = 0.0
    EPSYT(I) = EPSILONL
    BTPP(I) = SIGMAT-HT*EPSILONL
  END IF
  600 CONTINUE

  *****

```

```

C      CALCULATE STRAINS FOR SECOND DEFORMATION STAGE OF
C      THE FLEXIBLE ADHEREND
C      *****
C
C      DO 80 K=1, NS+1
C          EPS2(K, 1)= EPS1(K, NBETA+1)
C      80 CONTINUE
C      DO 90 K=1, NTHETA+1
C          THETAX(K)= THETAF*(K-1)/NTHETA
C          F(K)= FP/EXP((THETAF-THETAX(K))*FRICTION)
C      90 CONTINUE
C
C      EA(1)= EA(NBETA+1)
C
C      DO 100 K=2, NTHETA+1
C
C      CALL EAEFF2(EA, B, DS, NS, K, EC, ET, HT, EPS2, CRESSTRAIN, EPSYT)
C
C      DO 100 L=1, NS+1
C          EPS2(L, K) = EPS2(L, K-1)+(F(K)-F(K-1))/EA(K)
C      100 CONTINUE
C
C      *****
C      CALCULATE INCREMENTAL STRAIN ENERGY DENSITY FOR THE
C      SECOND DEFORMATION STAGE OF THE FLEXIBLE ADHEREND
C      *****
C
C      DO 120 N=1, NTHETA
C      DO 110 M=1, NS+1
C
C      IF (EPS2(M, N+1).LT. 0.0) THEN
C          IF (EPS2(M, N+1).LT. CRESSTRAIN(M)) THEN
C              DU(M)=(EC/2.)*(EPS2(M, N+1)**2.-EPS2(M, N)**2.)
C              * +BC(M)*(EPS2(M, N+1)-EPS2(M, N))
C          ELSE
C              IF (EPS2(M, N+1).LE. EPSYT(M)) THEN
C                  DU(M)=(ET/2.)*(EPS2(M, N+1)**2.-EPS2(M, N)**2.)
C                  * +BTP(M)*(EPS2(M, N+1)-EPS2(M, N))
C              ELSE
C                  DU(M)=(HT/2.)*(EPS2(M, N+1)**2.-EPS2(M, N)**2.)
C                  * +BTTP(M)*(EPS2(M, N+1)-EPS2(M, N))
C              END IF
C          END IF
C      ELSE
C          IF (EPS1(M, NBETA+1).LT. 0.0) THEN
C              IF (EPS2(M, N+1).GT. EPSYT(M)) THEN
C                  DU(M)=(HT/2.)*(EPS2(M, N+1)**2.-EPS2(M, N)**2.)
C                  * +BTTP(M)*(EPS2(M, N+1)-EPS2(M, N))
C              ELSE
C                  DU(M)=(ET/2.)*(EPS2(M, N+1)**2.-EPS2(M, N)**2.)
C                  * +BTP(M)*(EPS2(M, N+1)-EPS2(M, N))
C              END IF
C          ELSE
C              IF (EPS2(M, N+1).GT. EPSILONT) THEN
C                  DU(M)=(SIGMAT*(1-HT/ET)+(HT/2.)*(EPS2(M, N+1)+
C                  * EPS2(M, N)))*(EPS2(M, N+1)-EPS2(M, N))
C              ELSE
C                  DU(M)=(ET/2.)*(EPS2(M, N+1)**2.-EPS2(M, N)**2.)
C              END IF
C          END IF
C      END IF
C
C      110 CONTINUE

```

```

C
C *****
C   CALCULATE WORK/UNIT LENGTH FOR SECOND DEFORMATION STAGE
C   OF THE FLEXIBLE ADHEREND
C *****
C
C   U2=0.
C
C   CALL TRAPRULE(U2, DS, NS, DU)
C
C   U2=U2*B
C   W2=W2+U2
C
C 120 CONTINUE
C
C *****
C   CALCULATE UNLOADING/RELOADING STRESS-STRAIN PATHS FOR PORTION
C   OF THE ADHEREND YIELDED IN TENSION
C *****
C
C   DO 210 I=1, NS+1
C     IF (EPS2(I, NTHETA+1).GT. EPSYT(I)) THEN
C       SIGMAXT(I) = SIGMAT+(EPS2(I, NTHETA+1)-EPSYT(I))*HT
C       SIGRYC(I) = SIGMAXT(I)-(SIGMAT+SIGMAC)
C       BT(I) = SIGMAXT(I)-ET*EPS2(I, NTHETA+1)
C       TRESSTRAIN(I)= -BT(I)/ET
C       BCP(I) = -EC*TRESSTRAIN(I)
C       EPSYC(I) = (SIGRYC(I)-BCP(I))/EC
C       BCPP(I) = SIGRYC(I)-HC*EPSYC(I)
C     ELSE
C       BT(I) = 0.0
C       TRESSTRAIN(I)= 0.0
C       BCP(I) = 0.0
C       EPSYC(I) = EPSILONC
C       BCPP(I) = -SIGMAC-HC*EPSILONC
C     END IF
C 210 CONTINUE
C
C   DO 220 L=1, NS+1
C     RESSTRAIN(L)=0.0
C     IF (CRESSTRAIN(L).NE. 0.0) RESSTRAIN(L)=CRESSTRAIN(L)
C     IF (TRESSTRAIN(L).NE. 0.0) RESSTRAIN(L)=TRESSTRAIN(L)
C 220 CONTINUE
C
C *****
C   CALCULATE STRAINS FOR THIRD DEFORMATION STAGE OF THE
C   FLEXIBLE ADHEREND
C *****
C
C   DO 230 I=1, NS+1
C     EPS3(I, NBETA+1)=EPS2(I, NTHETA+1)
C 230 CONTINUE
C
C   DO 250 M=NBETA+1, 2, -1
C
C     DO 240 N=1, NS+1
C       EPS3(N, M-1)=EPS3(N, M)+(BETA(M-1)-BETA(M))*S(N)
C 240 CONTINUE
C 250 CONTINUE
C
C *****
C   CALCULATE INCREMENTAL STRAIN ENERGY DENSITY FOR SECOND
C   DEFORMATION STAGE OF FLEXIBLE ADHEREND

```

```

C*****
C
DO 330 M=NBETA+1,2,-1
DO 320 N=1,NS+1
IF(RESSTRAIN(N).GE.0.0) GOTO 300
IF(EPS3(N,M-1).LT.RESSTRAIN(N)) THEN
DU(N)=(EC/2.)*(EPS3(N,M-1)**2.-EPS3(N,M)**2.)
#
+BC(N)*(EPS3(N,M-1)-EPS3(N,M))
ELSE
IF(EPS3(N,M-1).LE.EPSYT(N)) THEN
DU(N)=(ET/2.)*(EPS3(N,M-1)**2.-EPS3(N,M)**2.)
#
+BTP(N)*(EPS3(N,M-1)-EPS3(N,M))
ELSE
DU(N)=(HC/2.)*(EPS3(N,M-1)**2.-EPS3(N,M)**2.)
#
+BTPP(N)*(EPS3(N,M-1)-EPS3(N,M))
END IF
END IF
GOTO 320
300 IF(RESSTRAIN(N).GT.0.0) GOTO 310
IF(EPS3(N,M-1).LT.0.0) THEN
DU(N)=(EC/2.)*(EPS3(N,M-1)**2.-EPS3(N,M)**2.)
ELSE
DU(N)=(ET/2.)*(EPS3(N,M-1)**2.-EPS3(N,M)**2.)
END IF
GOTO 320
310 IF(EPS3(N,M-1).GT.RESSTRAIN(N)) THEN
DU(N)=(ET/2.)*(EPS3(N,M-1)**2.-EPS3(N,M)**2.)
#
+BT(N)*(EPS3(N,M-1)-EPS3(N,M))
ELSE
IF(EPS3(N,M-1).GE.EPSYC(N)) THEN
DU(N)=((EC/2.)*(EPS3(N,M-1)**2.-EPS3(N,M)**2.)
#
+BPC(N)*(EPS3(N,M-1)-EPS3(N,M)))
ELSE
DU(N)=(HC/2.)*(EPS3(N,M-1)**2.-EPS3(N,M)**2.)
#
+BPCP(N)*(EPS3(N,M-1)-EPS3(N,M))
END IF
END IF
320 CONTINUE
C
C*****
C CALCULATE WORK/UNIT LENGTH FOR THIRD DEFORMATION STAGE
C OF THE ADHEREND
C*****
C
U3=0.0
C
CALL TRAPRULE(U3,DS,NS,DU)
C
U3=U3*B
W3=W3+U3
C
330 CONTINUE
C
C*****
C CALCULATE THE TOTAL WORK/UNIT LENGTH TO DEFORM THE
C FLEXIBLE ADHEREND AND TO FAIL THE ADHESIVE
C*****
C
WORK = W1+W2+W3
WORKADS = FP-WORK
ASTM = WORKADS/B
IF(FP.NE.0.0) THEN

```

```

      PERADH = WORK*100/FP
      PERADS = WORKADS*100/FP
END IF

```

```

C      WRITE(NOUT,333)WORK,WORKADS,PERADH,PERADS,ASTM
333 FORMAT(//1X,'*****',/26X,'O U T P U T',
#      '*****',/5X,
#      'D A T A',/1X,'*****',
#      '*****',/5X,
#      'WORK/UNIT LENGTH TO DEFORM ADHEREND (in-lb/in) = ',F6.2,
#      /5X,'WORK/UNIT LENGTH TO FAIL ADHESIVE (in-lb/in) = ',F6.2,
#      /5X,'% OF TOTAL WORK TO DEFORM ADHEREND = ',F5.1,
#      /5X,'% OF TOTAL WORK TO FAIL ADHESIVE = ',F5.1,
#      /5X,'ASTM PEEL STRENGTH (lb/in. width) = ',F6.2)

```

```

C      STOP
      END

```

```

C*****

```

```

      SUBROUTINE EAEFF1(EPSILONC,EPSILONT,HC,EC,ET,HT,B,DS,
#      NS,EA,M,XSTR)
      PARAMETER (NX=505)
      IMPLICIT DOUBLE PRECISION (A-H,O-Z)
      DIMENSION E(NX),XSTR(NX),EA(NX)
      DO 40 I=1,NS+1
        IF(XSTR(I).GE.EPSILONC) GOTO 10
        E(I)=HC
        GOTO 40
10      IF(XSTR(I).GE.O.O) GOTO 20
        E(I)=EC
        GOTO 40
20      IF(XSTR(I).GT.EPSILONT) GOTO 30
        E(I)=ET
        GOTO 40
30      E(I)=HT
40      CONTINUE
      EAEFF=0.0

```

```

C      CALL TRAPRULE(EAEFF,DS,NS,E)

```

```

C      EA(M)=B*EAEFF
      RETURN
      END

```

```

C*****

```

```

      SUBROUTINE EAEFF2(EA,B,DS,NS,K,EC,ET,HT,XSTR,RSTR,YSTR)
      PARAMETER (NX=505,N1=105)
      IMPLICIT DOUBLE PRECISION (A-H,O-Z)
      DIMENSION E(NX),XSTR(NX,N1),RSTR(NX),
#      YSTR(NX),EA(NX)
      DO 10 L=1,NS+1
        IF(XSTR(L,K-1).LT.RSTR(L)) THEN
          E(L)=EC
        ELSE
          IF(XSTR(L,K-1).GT.YSTR(L)) THEN
            E(L)=HT
          ELSE
            E(L)=ET
          END IF
        END IF
10      CONTINUE
      EAEFF=0.0

```

```

C      CALL TRAPRULE(EAEFF,DS,NS,E)

```

C

```
EA(K)=B*EAEFF  
RETURN  
END
```

C*****

```
SUBROUTINE TRAPRULE(X,DX,N,XARR)  
PARAMETER ( NX = 505 )  
IMPLICIT DOUBLE PRECISION (A-H,O-Z)  
DIMENSION XARR(NX)  
DO 10 I=1,N  
    X=X+XARR(I)+XARR(I+1)  
10 CONTINUE  
X=X*DX/2.  
RETURN  
END
```


APPENDIX B

GUIDELINES FOR USE OF UDRI FIXTURE

The UDRI peel test fixture is a modified version of the fixture illustrated in ASTM D3167 and was designed to accommodate various adherend and adhesive thicknesses. It was also designed to constrain the test specimen and force it to deform to the geometry of the roller. In the peel test, the contact angle is approximately 116.5° . Figure 16 presents a schematic diagram of the UDRI peel test fixture and Figure 17 presents details for the side plate.

To adjust the position of the rollers, follow the procedure listed below.

(1) To adjust roller 1, place a test specimen in the fixture so that it contacts rollers 2 and 3. Adjust the set screws such that a shim (equal to the sum of the flexible adherend thickness and adhesive thickness) can be placed between the specimen and bearing 1.

(2) To position roller 4, adjust the set screws such that a shim of specified thickness can be placed between rollers 2 and 4. The specified thickness of the shim should equal the sum of the flexible adherend thickness, the adhesive thickness, and a clearance factor of 0.005 inch.

(3) Tighten the appropriate bolts to secure the fixture, making sure the bolts are in contact with the set screws. It is not critical to secure the bolt which supports bearing 4. The analyst need only adjust the fixture when the adherend and/or adhesive thickness changes.

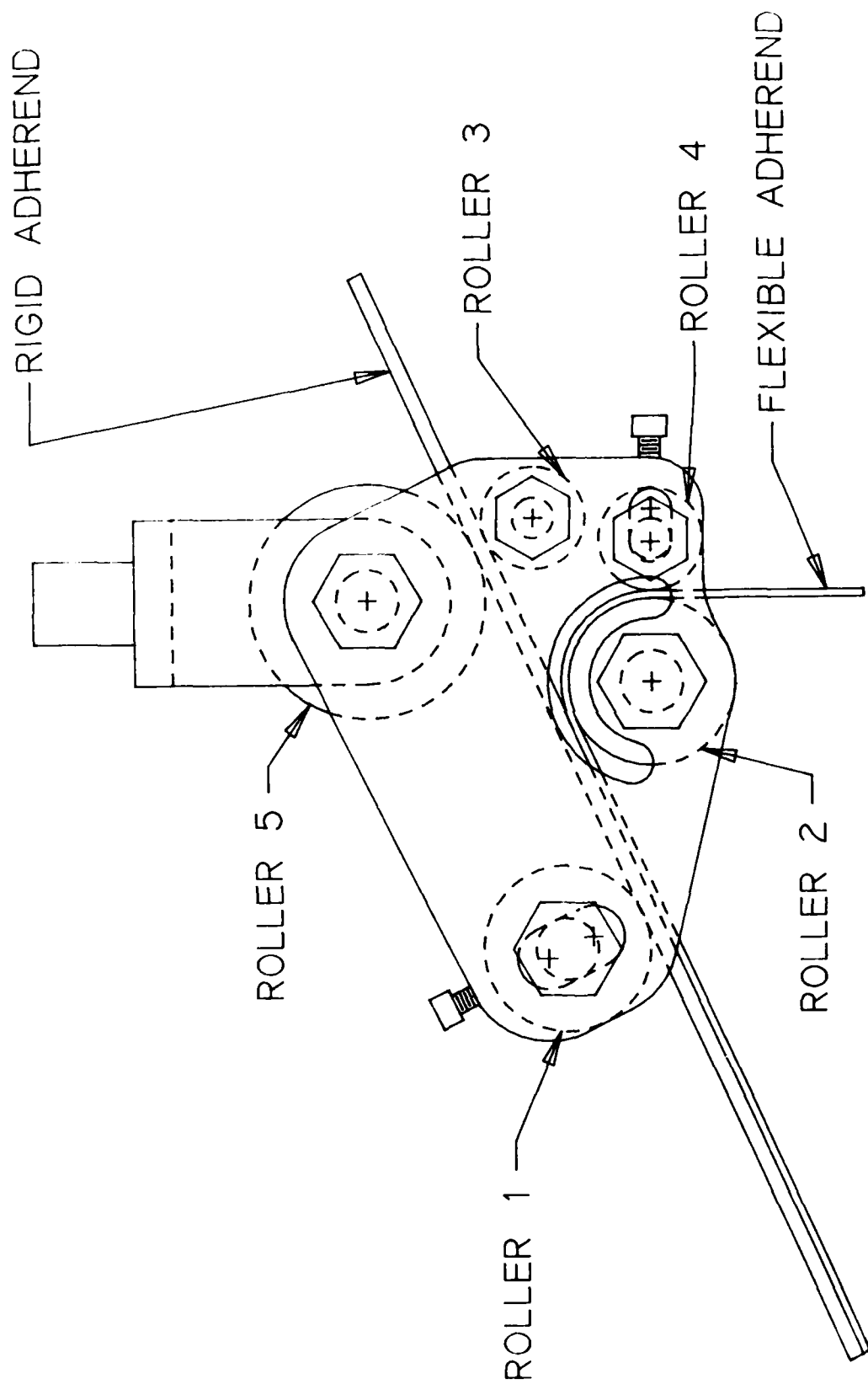


FIGURE 16 - UDRI TEST FIXTURE

END

DATE

FILMED

8-88

OTIC